FRONTIERS OF PHYSICS

TOPICAL REVIEW
Volume 17 / Issue 3 / 31504 / 2022

Understanding the mechanisms of brain functions from the angle of synchronization and complex network

Tianwei Wu[1], Xinhua Zhang[2], Zonghua Liu[1,†]

1 School of Physics and Electronic Science, East China Normal University, Shanghai 200241, China
2 Jinhua Middle School, Shanghai 200333, China
Corresponding author. E-mail: †zhliu@phy.ecnu.edu.cn
Received February 14, 2022; accepted March 31, 2022

ABSTRACT

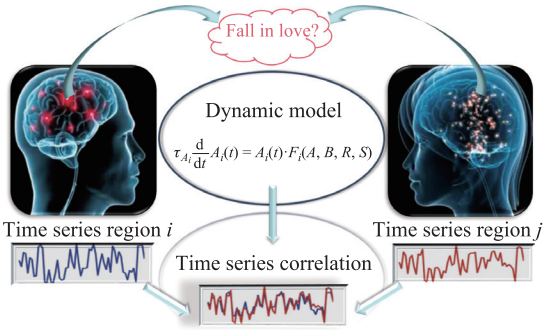

The human brain is the most complicated and fascinated system and executes various important brain functions, but its underlying mechanism is a long-standing problem. In recent years, based on the progress of complex network science, much attention has been paid to this problem and many important results have been achieved, thus it is the time to make a summary to help further studies. For this purpose, we here make a brief but comprehensive review on those results from the aspect of brain networks, i.e., from the angle of synchronization and complex network. First, we briefly discuss the main features of human brain and its cognitive functions through synchronization. Then, we discuss how to construct both the anatomical and functional brain networks, including the pathological brain networks such as epilepsy and Alzheimer's diseases. Next, we discuss the approaches of studying brain networks. After that, we discuss the current progress of understanding the mechanisms of brain functions, including the aspects of chimera state, remote synchronization, explosive synchronization, intelligence quotient, and remote propagation. Finally, we make a brief discussion on the envision of future study.

Keywords brain functions, complex network, synchronization, chimera state, remote synchronization, explosive synchronization, intelligence quotient, remote propagation

Contents

1 Brief introduction of the human brain and its cognitive functions

It is well known that the human brain is the most complicated and fascinated system and is usually considered as a "black" box, thus its underlying mechanism has always been the most interesting topic. Based on the development of modern physical techniques such as the electroencephalography (EEG), magnetoencephalography (MEG), and functional magnetic resonance imaging (fMRI) tech-

https://doi.org/10.1007/s11467-022-1161-6

niques, this system is now becoming not so "black" anymore. Especially, based on the progress of complex network science, many significant results on brain networks have been achieved. However, these achievements are only a tip of the iceberg and more tasks await us. For example, both the human brain and Internet are complex networks, with the former being part of nature and the latter being created by man, but they work very differently and each one surpasses the other in certain types of information processing. On the one hand, we can fast recognize the face and the voice of a friend in an unordered crowd, but the Internet cannot. On the other hand, a computer connected to Internet can quickly find a relevant page on the World Wide Web among millions of pages, but the human brain cannot. More examples can be found in the aspects of consciousness and memory. In this sense, we here make this brief review to help future studies, which is only mainly focused on the results from the angle of synchronization and complex network as the brain network is basically a networked dynamical system.

General speaking, the human brain is thought to be a distributed information processing device and has obtained an increasing interest in recent years. We know that the human brain looks like a walnut and its size is about a pomelo. The weight of human brain is about 1.4 kilograms, i.e., 2% of human body, but consumes about 20% of the body's energy. The surface of the cerebral cortex is folded into many convolutions, resulting in a complex anatomical configuration that has long been thought to increase cortical surface area while conserving axonal volume. The brain network consists of 10^{11} neurons connected by 10^{15} synapses, with 80% excitatory neurons (i.e., pyramidal cells) and 20% inhibitory neurons (i.e., interneurons). These neurons are heterogeneously distributed on the brain network and can be divided into different communities, thus the human brain consists of complicated neural circuits with multiple spatial scales [1]. That is, it is about $\sim$ 10 cm at the level of whole brain, $\sim$ 1 cm at the level of cortical areas, 100 μm – 1 mm at the level of local network, 10 μm – 1 mm at the level of neuron, 100 nm – 1 μm at the level of sub-cellular compartments, and $\sim$ 10 nm at the level of channel, receptor, and intracellular protein. This topological feature of multiple spatial scales is a key element of human brain and is also the source of our strong ability on the aspects of memory and cognitive functions. By this feature, the brain network can generate multiple temporal scales of the brain, such as the days-years of long-term memory, seconds–minutes of short-term (working) memory, 100 ms – 1 s of behavioral time scales/reaction times, $\sim$ 10 ms of single neuron/synaptic time scales, $\sim$ 1 ms of action potential duration/local propagation delays, and $\ll$ 1 ms of channel opening/closing.

Another key feature of human brain is its self-organized criticality (SOC) [2, 3]. In the state of SOC, cortical networks exhibit diverse patterns of activity, including oscillations, synchrony, and waves *etc.*, thus the dynamic behaviors can occur in various spatial and temporal scales, which is the basis for us to study the dynamic response of human brain network at different scales. This sate of SOC also makes our brain system have super computing capability. On the other hand, plasticity is also one of the most astonishing features of the brain and can be defined as the ability to modify the structural and functional properties of synapses [4, 5]. Among the postulated mechanisms of synaptic plasticity, the activity-dependent Hebbian plasticity constitutes the most fully developed and influential model of how information is stored in neural circuits [6, 7].

Based on these features, the brain networks can be classified into two kinds of networks, i.e., the structural and functional brain networks, where the former is relatively well studied and the latter is still in progress. For the structural network, it can be further divided into different subnetworks, according to its feature of multiple spatial scales. Roughly speaking, we may divide the brain network into two levels. The first level is the two hemispheres connected by corpus callosum. And the second level is the nine cognitive subnetworks named as auditory (Aud), visual (V), motor and somatosensory (MS), ventral temporal association (VT), attention system (Att), medial default mode (mDm), cingulo-opercular (CO), and frontoparietal (FP) systems, where each cognitive system is defined by regions that coactivate in support of a generalized class of cognitive functions [8].

For the functional network, it reflects the dynamic interaction of functionally specialized but widely distributed cortical regions and is obtained by the Pearson correlation coefficients between the measured EEG time series [1]. There are strong evidences that synchronization of neural activity, both locally and between distant regions, is a crucial code for functional interactions. To understand how the different neuronal groups interact with each other and how their communication is flexibly modulated to bring about our cognitive dynamics, an assumption is that neuronal communication is mechanistically subserved by neuronal coherence [9]. In this sense, there will be a strong correlation or synchronization among these cooperated neurons and make them form a synchronized network, thus each brain function will correspond to a specific brain functional network. Many evidences have been found for this relationship between synchronization and brain functions. For example, long-range synchronization of oscillatory signals has been suggested to mediate the interactions within large-scale cortical networks [10]. Invasive recordings reveal task-specific synchronization between pairs of focal cortical sites [11]. EEG and MEG measure synchronized signals across widely distant extracranial sensors [12]. Synchronous neural firing at the gamma frequency might be the neural correlate of visual awareness [13]. And the activity of slow waves in sleep synchronizes cortical regions with high temporal precision and can recruit multiple subcortical targets [14]. Therefore, synchronous neural oscillations reveal much about the origin and nature of cognitive processes such as mem-

ory, attention and consciousness. Moreover, specific oscillations have been identified with particular cognitive processes: theta and gamma rhythms with memory encoding and retrieval, alpha and gamma rhythms with attentional suppression and focusing, and global synchronization at the gamma frequency with consciousness, etc. [15]. Therefore, most of fundamental cognitive processes are closely related to the synchronous activity of neurons in the brain.

2 Basic concepts of complex networks

As pointed out above, a brain network consists of a huge number of neurons (10^{11}) and connections (10^{15}), thus its structure is very complicated and can be described at different levels [16]. At the fundamental level, local neurons form microcircuits, often arranged in a modular architecture. These different microcircuits will be connected each other to form a global brain network. At the middle level, a number of neurons (i.e., thousands or even more) will be considered as a node and a fraction of all the nodes will form a cognitive subnetwork. These different cognitive subnetworks will execute different brain functions. While at the global level, all the nodes will form a globally connected network. Figure 1 shows a schematic figure of brain network.

Obviously, Fig. 1 is a typical complex network, thus the approaches of complex networks may be applied to study brain networks. In fact, this is what we have done as the first step to understand the brain network. So far, we have known that the brain network is unique and has its own characteristic features such as the community, rich club, hub, and core. Figure 2 shows such a schematic figure.

Based on these characteristic features of Figs. 1 and 2, we can make further studies of brain network such as the dynamics, relationship with brain functions, and even pathological disorders. They are what we will gradually introduced in the following sections. But here, as a preparation, we would like to briefly introduce some basic concepts of complex networks to help us to roughly understand the brain network.

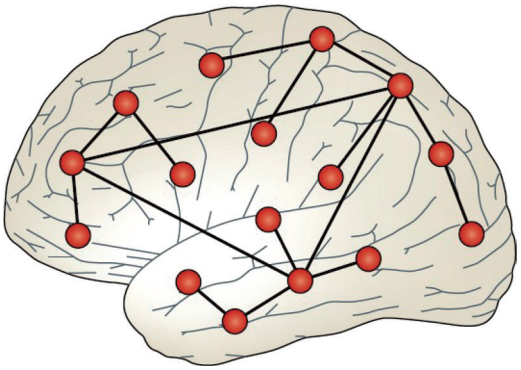

Fig. 1 A schematic figure of brain network where the red "circles" represent the network nodes and the solid lines represent the network connections. Reproduced from Ref. [16].

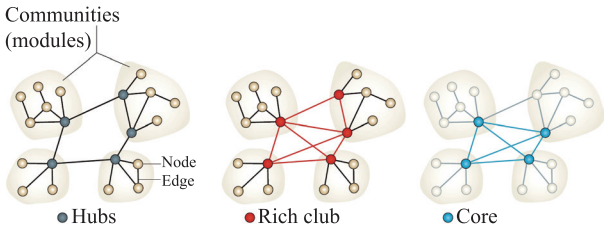

Fig. 2 Some characteristic features of brain network such as the community, rich club, hub, and core. Reproduced from Ref. [16].

Node degree: The degree of a node is the sum of its incoming (afferent) and outgoing (efferent) connections. The number of afferent and efferent connections is also called the "in-degree" and "out-degree", respectively.

Degree distribution: The degrees of all the network's nodes form a degree distribution. In random networks all connections are equally probable, resulting in a Gaussian and symmetrically centred degree distribution. Complex networks generally have non-Gaussian degree distributions, often with a long tail towards high degrees. The degree distributions of scale-free networks follow a power law.

Hub: A node with higher node degree or larger betweenness centrality. Hubs play an important role in information integration in a network.

Path length: Path length is the minimum number of edges that must be traversed to go from one node to another. Random and complex networks have short mean path lengths whereas regular lattices have long mean path lengths.

Efficiency: Efficiency is inversely related to path length but is numerically easier to use to estimate topological distances between elements of disconnected graphs.

Betweenness centrality: Betweenness centrality is a measure of the extent to which a node acts as a bridge that creates the shortest path between two other nodes.

Assortativity: Assortativity is the correlation between the degrees of connected nodes. Positive assortativity indicates that higher degree nodes tend to connect to each other. While disassortativity or negative assortativity indicates that higher degree nodes tend to lower degree nodes.

Module: Each module contains several densely interconnected nodes, and there are relatively few connections between nodes in different modules.

Community structure: The sub-global organization of a complex network. Modularity is an example of community structure, but not all network communities are simply modular.

Rich club: A rich club is of densely inter-connected hubs that has a central role in generating globally efficient information flow.

Robustness: The degree to which the topological

properties of a network are resilient to "lesions" such as the removal of nodes or edges.

Global efficiency: Global efficiency is the inverse of average shortest path lengths over all pairs of nodes. This measure reflects the capacity of global integration of a network.

Adjacency matrix: An adjacency matrix is an $N \times N$ matrix with entries $a_{ij} = 1$ if node j connects to node i, and $a_{ij} = 0$ if there is no connection from node j to node i.

Clustering coefficient: The clustering coefficient C_i of a node i is calculated as the number of existing connections between the node's neighbors divided by all their possible connections. The clustering coefficient ranges between 0 and 1 and is typically averaged over all nodes of a network to yield the network's clustering coefficient C.

3 Construction of the structural and functional brain networks

The ultimate goal of human brain research is to understand the neural basis of human behavior, so as to provide theoretical basis for a profound understanding of human intelligence, improving the efficiency of human brain, accurate diagnosis and treatment of various neurological diseases and mental diseases. For this goal, much attention has been paid to the construction of the structural and functional brain networks as they are the key elements to study brain functions. In this section, we briefly discuss how to detect or construct the structural and functional brain networks. We first focus on the case of the structural brain network.

For the brain network with 10^{11} neurons and 10^{15} synapses, it is very difficult to experimentally measure the brain structure network at the level of neurons, thus an available brain network has to be a simplified one. In this sense, an alternative approach is to estimate the anatomical connectivity by the technique of diffusion spectrum imaging (DSI), which is the set of physical or structural (synaptic) connections linking neuronal units at a given time [17]. Anatomical connectivity data can range over multiple spatial scales, from local circuits to large-scale networks of inter-regional pathways, i.e., mesoscale maps of anatomical brain connectivity. Anatomical connection patterns are relatively static at shorter time scales (seconds to minutes), but can be dynamic at longer time scales (hours to days). The upper-left of Fig. 3(a) shows such an example by DSI. We see that it is still very large and complicated at the level of mesoscale, although it is much simplified than the brain structure network at the level of neurons.

A further simplification step is to divide the human brain into different regions of interests (ROIs) and consider each ROI as a network node [17]. In this framework of network, each network edge represents the strength of the connection between two brain regions, i.e., a weighted connectivity. The lower part of Fig. 3(a) shows the resulted network with 234 nodes. It is now a typical complex network and can be conveniently used to study the brain dynamics.

How to define these ROIs, i.e., brain parcellation, is a key problem in the construction of brain network [18], which depends on the spatial heterogeneity of brain organization or the multiple topographies at different scales. A basic condition is that the constructed brain network comprises multiple discontinuous but closely interacting regions, which is fundamental for understanding brain organization and function. Moreover, a wealth of different features should be considered, ranging from local properties of brain tissue to long-range connectivity patterns, in addition to structural and functional markers. In fact, brain cartography has a long history, over which different properties of brain tissues have been progressively integrated towards the now commonly accepted conceptualization of brain areas as entities that show distinct connectivity, microarchitecture, topography and function [19]. More specifically, properties of these features regularly reveal zones of homogeneity and abrupt changes between zones, such as the thickness of cortical layers, the size of pyramidal cells or the extent of myelination. Two conceptually distinct approaches are the boundary mapping and clustering or factorization, which are referred to as local partitioning and global partitioning approaches, respectively. In the boundary mapping approach, a border is detected by localizing the most abrupt spatial changes in the assessed feature using a local border detection technique. In clustering and factorization approaches, spatial elements (voxels or vertices) are grouped on the basis of their similarity and dissimilarity according to a given marker. Clustering is used to group similar voxels or vertices together and apart from different voxels or vertices, whereas factorization organizes the data sets into dimensions and components that best represent variations in the data. Importantly, all methods have distinct advantages and disadvantages, and thus the choice of approach should

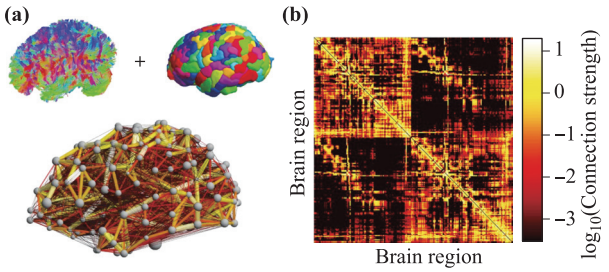

Fig. 3 Schematic figure for the construction of the structural brain network. **(a)** The brain connectivity is obtained by combining tractography estimates from diffusion spectrum imaging data of a specific individual's brain and a parcellation of the brain into 234 regions. **(b)** The resulting anatomical connectivity matrix where entries indicate the density of connections between two brain regions. Reproduced from Ref. [17].

depend on the data at hand, as well as the objective of the parcellation.

Accordingly, the upper-right of Fig. 3(a) shows such a parcellation. Combining the two parts of the upper-left and upper-right of Fig. 3(a) gives the network of the lower part of Figs. 3(a) and (b) shows the resulting anatomical connectivity matrix where entries indicate the density of connections between two ROIs. From Fig. 3(b) we see that its structure is of the properties of small-world topology, highly connected hubs and modularity.

As an example, we use the data of Refs. [18, 20] to construct a brain network. In this data, the cerebral cortex was divided into relatively uniform 998 ROIs with each representing a network node, and the connections in all possible pairs of 998 ROIs were measured noninvasively by using DSI. In this way, a connection between two ROIs was derived from the number of fibers found by the tractography algorithm, which results in 17865 connections and 9 isolated nodes without detected fibers due to resolution limitation of DSI. Furthermore, the cerebral cortex can be parcellated into 66 functional regions [18, 20]. In this work, we remove the 9 isolated nodes, leaving $N = 989$ nodes, with $N_r = 496$ nodes in the right hemisphere and $N_l = 493$ nodes in the left hemisphere. The number of cortical regions covered by these nodes is also reduced to 64. The obtained 989×989 connection matrix is actually weighted, with the connection weights representing the fiber density between the connected nodes. To clearly see the cortical regions, we put all the 989 nodes on a circle and number them from one cortical area to another one. We find that the 64 regions are equally distributed on the left and right hemispheres, i.e., 32 on the left hemisphere and 32 on the right hemisphere. We label the nodes in each region consecutively. Then, we put the 17865 links correspondingly into the circle [21]. In this way, the links in the same cortical region, between different regions, and between the left and right hemispheres will not be overlapped, so that it is clear to see how the cortical regions are connected. Figure 4 shows the topology where the names of anatomical cortical regions are labeled on the circle and the green, blue and red lines represent the links among the nodes within cortical regions, between different regions, and between the left and right hemispheres, respectively.

There has been more and more evidences that brain networks, ranging from simple nets of interconnected neurons up to macroscopic networks of brain areas, display the typical features of complex systems: high clustering, short path lengths, skewed degree distributions, presence of hubs, assortative mixing and the presence of modules [22].

In contrast to the structure brain network, the functional brain network is not static but time-dependent (hundreds of milliseconds) and "model-free". The concept of functional connectivity refers to the statistical interdependencies between physiological time series recorded in various brain areas, and is thought to reflect communica-

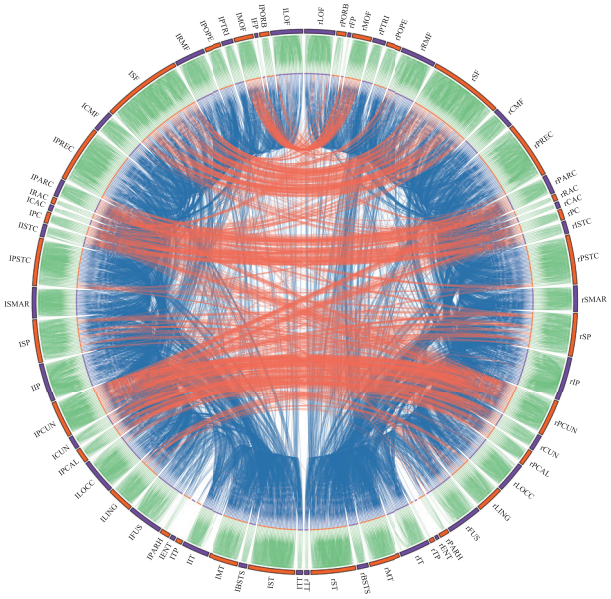

Fig. 4 The network topology of the 64-region parcellation for the network of cerebral cortex with 989 nodes and 17865 links, where the names of functional brain regions are put on the circle and the green, blue and red lines represent the links within cortical region, between different regions, and between the left and right hemispheres, respectively. Reproduced from Ref. [21].

tion between several brain areas [23]. MEG is a method used to assess functional connectivity within the brain. The functional connectivity between each pair of channels represents a link whose weight reflects the strength of the connectivity or correlation. Regardless of the modality of recording activity (EEG, MEG, or fMRI), topological features of functional brain networks are defined over long periods of time, neglecting possible instantaneous time-varying properties of the topologies. Thus, a functional brain network is created by regarding each MEG channel as a node, which may be based on reconstructed anatomical ROIs. However, different methodologies of measuring brain activity will generally result in different statistical estimates of functional connectivity [24–27]. On the other hand, it is increasingly evident that brain regions are continuously interacting even when the brain is "at rest" and, more importantly, that the functional networks uncovered from resting data closely match those derived from a wide variety of different activation conditions.

In fact, attempts to track the functional connectivity of the brain have a long history. The Dutch neuroscientist Barenne used strychnine-induced disinhibition to track functional interactions in the macaque cerebral cortex [22]. Many years later, Stephan *et al.* [28] collected data from the literature to reconstruct the functional network of primate cortex. However, it should be stressed that this study was based on purely historical data, and that the concept of functional connectivity was rather indirect since it was not based upon the direct observa-

tion of correlated or synchronized electrical activity in distant neuronal populations. A more direct observation was made by Bettencourt *et al.* [29] who looked at the spiking activity of cultured neuronal cell assemblies. After that, various techniques have been used to construct the functional brain networks.

As an example, we follow Eguiluz *et al.* to show how to extract functional networks and analyze them in the context of the current understanding of complex networks [24]. Their approach is the following. For a given task, at each time step, magnetic resonance brain activity is measured in $36 \times 64 \times 64$ brain sites. The activity of voxel x at time t is denoted as $V(x,t)$. Two voxels are defined as functionally connected if their temporal correlation exceeds a positive predetermined value r_c, regardless of their anatomical connectivity. Then, the linear correlation coefficient between any pair of voxels, x_1 and x_2, can be calculated as

$$r(x_1,x_2) = \frac{\langle V(x_1,t)V(x_2,t)\rangle - \langle V(x_1,t)\rangle\langle V(x_2,t)\rangle}{\sigma(V(x_1))\sigma(V(x_2))}, \tag{1}$$

where $\sigma^2(V(x)) = \langle V(x,t)^2\rangle - \langle V(x,t)\rangle^2$, and $\langle\cdot\rangle$ represents temporal averages.

Figure 5 shows how underlying functional networks are exposed during any given task. Top four images represent snapshots of activity and the three traces correspond to selected voxels from visual (V1), motor (M1) and posterioparietal (PP) cortices. The correlation matrix is calculated by Eq. (1) and then used to define the network among the highest correlated nodes. A crucial issue is the choice of threshold r_c. Different thresholds will generate graphs of different sparsity or connection density, and so network properties are often explored over a range of plausible thresholds.

While differences in brain connectivity have long been known to exist between diseased and healthy populations [17]. A hypothesis is that cognitive impairment in most brain pathologies is linked to the impact of the pathology on brain connectivity [30]. Besides the classical disconnection syndromes, almost all neurological or psychiatric disorders may be regarded as network dysconnections or deregulations. This is obvious for the diseases classically regarded as localized or global network pathologies such as epilepsy, autism spectrum disorders (ASD), schizophrenia or Alzheimer's disease (AD). For examples, it was assumed that the cognitive dysfunction in AD could be due, at least in part, to a functional disconnection between distant brain areas [31]. For a wide range of thresholds, the characteristic path length L was significantly longer in AD, whereas the cluster coefficient C showed no significant changes. That is, AD is characterized by a loss of small-world network characteristics. For the emergence of epileptic discharges, Chavez *et al.* [32] analyzed the connectivity structure of weighted brain networks extracted from spontaneous MEG signals of healthy subjects and epileptic patients recorded at rest. They found that, for the activities in the 5–14 Hz range, healthy brains exhibit a sparse connectivity, whereas the brain networks of patients display a rich connectivity with a clear modular structure. Further, the no-task fMRI data showed that people with schizophrenia tend to have a less strongly integrated, more diverse profile of brain functional connectivity, associated with a less hub-dominated configuration of complex brain functional networks [33]. Thus, these studies have opened new avenues for disease analysis. On brain imaging, the affected brain regions of Alzheimer's patients matched exactly the regions that make up the default mode neural network [30]. Thus, AD may one day be classified as a default mode neural network associated disease.

The approach of Eq. (1) is a symmetrical measure and can be generalized to asymmetrical measures of causal association or effective connectivity [34]. Unlike functional connectivity, effective connectivity is not "model-free", but requires the specification of a causal model including structural parameters. Experimentally, effective connectivity can be inferred through perturbations, or through the observation of the temporal ordering of neural events.

Importantly, structural, functional and effective connectivity are mutually interrelated [23]. Structural connectivity is a major constraint on the kinds of patterns of functional or effective connectivity. Structural inputs and outputs of a given cortical region are major determinants of its functional properties. Conversely, functional interactions can contribute to the shaping of the underlying anatomical substrate, either directly through activity-dependent synaptic modification, or, over longer time scales, through affecting an organism's perceptual, cognitive or behavioral capabilities, and thus its adaptation and survival.

4 Approaches of studying brain functions

Considering the fact that brain functions are based on neural synchronization, its study has gone through two stages in history: relationship between phase synchronization and brain functions and the partial synchronization of brain networks. In the first stage, the concepts of synchronization are well studied and various models of cognitive functions are proposed. Thus, the attention was mainly concentrated on principles of synchronization in cognitive processes such as the cognition and memory. While in the second stage, the attention is transferred to how the unique topology of real brain network influences its functions. We firstly discuss the first stage.

In this stage, many concepts of synchronization have been introduced such as complete synchronization, phase synchronization, delay synchronization, and generalized synchronization [35–37]. Among them, the phase synchronization is evidenced to have close relationship with brain functions and is thus a fundamental neural mechanism [38]. In human brain, phase synchronization refers

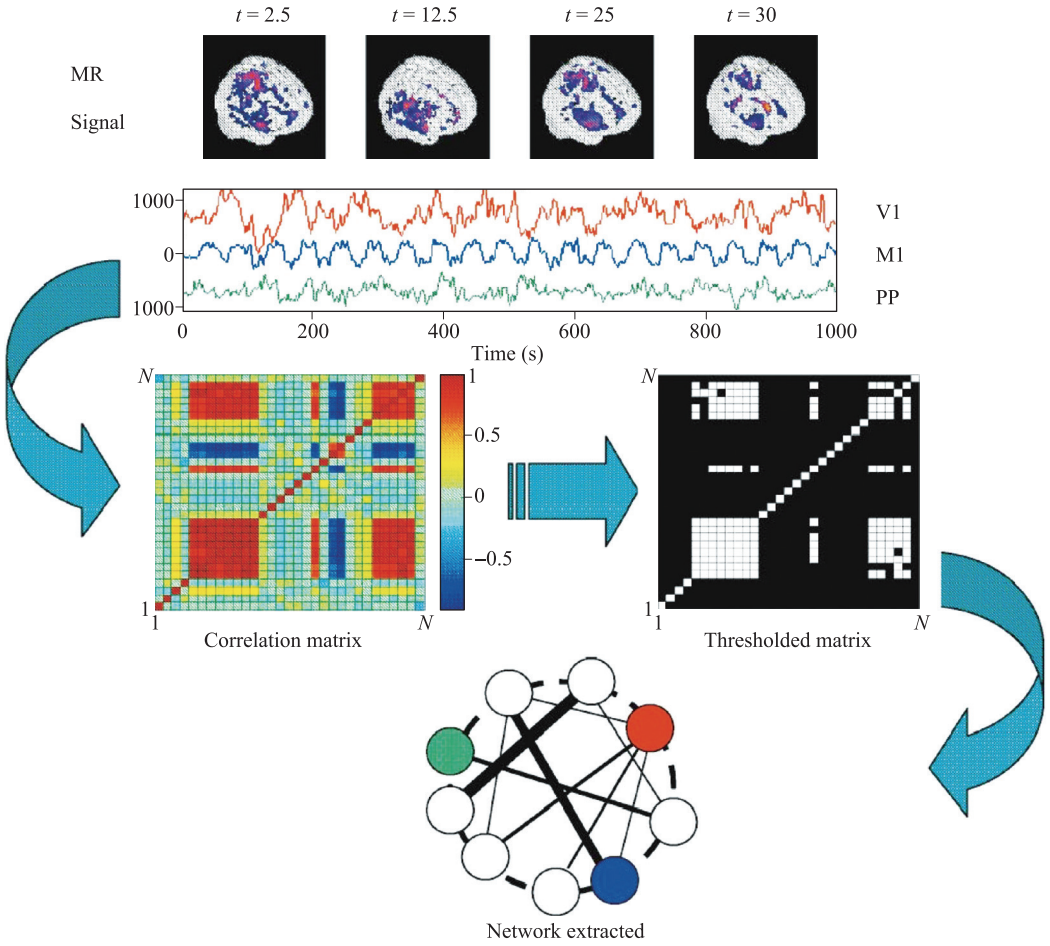

Fig. 5 Methodology used to extract functional networks from the signals. The correlation matrix is calculated and then used to define the network among the highest correlated nodes. Top four images represent snapshots of activity and the three traces correspond to selected voxels from visual (V1), motor (M1) and posterio-parietal (PP) cortices. Reproduced from Ref. [24].

to the synchronization of oscillatory phases between different brain regions. It supports neural communication and neural plasticity and is probably relevant for many cognitive processes. If synaptic connections between two regions are strengthened, phase synchronization will be more easily induced, and the two regions will be more likely to communicate with each other.

Phase synchronization supports two general functions, namely, neural communication and spike timing-dependent plasticity, thus phase synchronization takes important role in memory processes. Several human scalp EEG studies show that theta phase synchronization between the prefrontal cortex and the temporal lobe occurs not only during encoding and retrieval [39], but persists during the maintenance interval of working memory [40]. Interestingly, beta phase synchronization was accompanied by increases in the power (that is, the square of the EEG signal amplitude) of gamma oscillations in the visual cortex and in gamma phase synchronization in the medial temporal lobe [41].

In addition to phase synchronization of oscillations in different brain regions, other synchronization mechanisms facilitate the representation of multiple objects in memory. They include cross-frequency phase–amplitude coupling and cross-frequency phase–phase coupling [42]. Several studies suggest that phase–amplitude coupling supports multi-item working memory, for which it may be necessary to separate the representations of individual objects [42]. Phase synchronization can also occur between oscillations of different frequencies, an effect known as "$m:n$ phase synchronization" with $m \neq n$. The complementary mechanisms of phase–amplitude coupling and $m:n$ phase coupling are crucial for a non-interfering representation of multiple objects in working memory.

Figure 6 shows an integrative view of memory-related synchronization mechanisms [38]. It shows the schematic flow of how all three synchronization mechanisms are related to both working memory and long-term memory (and to the interaction between these memory processes). From this figure we see that phase synchronization supports two general functions — namely, neural communication and spike timing-dependent plasticity. In addition, phase synchronization probably supports object representation — for example, through feature binding. This func-

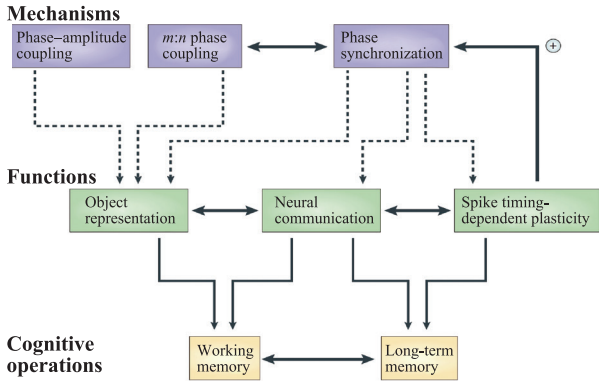

Fig. 6 An integrative view of memory-related synchronization mechanisms. In this schematic overview, dotted arrows point to the functions that are supported by the different neural mechanisms. Thin black arrows indicate that functions contribute to cognitive operations. Thick double-headed arrows represent interactions between mechanisms, functions or cognitive operations. Reproduced from Ref. [38].

tion also relies on neural communication (as indicated by the double-headed arrow). Neural communication facilitates both working memory and long-term memory processes, whereas spike timing-dependent plasticity specifically contributes to long-term memory.

In the second stage, our main task is to study the influence of network topology on synchronization and then to understand the mechanism of mind from the angle of brain networks. The brain is inherently a dynamic system, in which the traffic between regions, during behavior or even at rest, creates and reshapes continuously complex functional networks of correlated dynamics. Concerning dynamics, the performance of cognitive tasks can be considered as the emergence of spatiotemporal patterns of brain activity. Thus, understanding the dynamical patterns is a key to understand the mechanism of brain functions. For this purpose, a main assumption is that network structure and nodes dynamics make variety of brain functions [43]. That is, we assume

$$Network\ structure + Nodes\ dynamics = Brain\ functions.$$

To illustrate this idea in details, Fig. 7 shows its schematic diagram. We first extract the functional network from sequential fMRI signals. Then, we add a dynamic model on each network node, representing the activities $A_i(t)$ of the cognitive modes. After that, we figure out the optimal parameters in parenthesis by comparing the network outputs with the measured data of cognitive tasks. Finally, we use the network dynamics to predict cognitions and behaviors.

For such a brain network, a general way to study its dynamics is by letting each node be a neural oscillator such as the FitzHugh–Nagumo neuron or Hindmarsh-Rose neuron. However, this approach may be problematic as each node represents in fact the collective behaviors of thousands of neurons in an ROI, i.e., a mean-field. For an isolated node with thousands of neurons, we may expect two kinds of behaviors, i.e., high or low firing rates. For the former, the total input coupling to each neuron in a ROI is sufficiently high to fire, thus making the neurons of ROI insensitive to further input from other nodes. Consequently, the node may keep its state of high firing rate for a finite time. We call this state activation. While for the latter, the total input of each neuron in a ROI is insufficient to reach the threshold of firing, thus it is possible for the neurons of ROI to receive input from other nodes. We call this state inactivation. Thus, for two connected nodes in brain network, their interaction can be approximately classified into three cases: (i) There is no interaction between them when both nodes are in the state of inactivation. (ii) There is a firing transmission from the activated one to the inactivated one when one node is in the state of activation while the other is in the state of inactivation. The firing of inactivated node depends on the total input received from all its neighbors. (iii) The interaction will be small and can be ignored when both nodes are in the state of activation.

In mean-field, the dynamics of each node on the brain network can be modeled by nonlinear Wilson–Cowan oscillators (WCOs). The WCO is a biologically motivated model of local brain activity, developed to describe the mean behavior of small neuronal populations [44]. The model therefore simulates regional brain dynamics. In this biologically motivated model of neuronal populations, the fraction of excitatory and inhibitory neurons active at time t in the i-th brain region are denoted by $E_i(t)$ and $I_i(t)$, respectively, and their temporal dynamics are given by [17]

$$\begin{aligned}\tau\frac{\mathrm{d}E_i}{\mathrm{d}t} &= -E_i(t) + (S_{E_m} - E_i(t))S_E(c_1E_i(t) - c_2I_i(t) \\ &\quad + c_5\sum_j A_{ij}E_j(t-\tau_d^{ij}) + P_i(t)) + \sigma w_i(t), \\ \tau\frac{\mathrm{d}I_i}{\mathrm{d}t} &= -I_i(t) + (S_{I_m} - I_i(t))S_I(c_3E_i(t) - c_4I_i(t) \\ &\quad + c_6\sum_j A_{ij}I_j(t-\tau_d^{ij})) + \sigma v_i(t),\end{aligned} \tag{2}$$

where

$$S_{E,I}(x) = \frac{1}{1+\mathrm{e}^{-a_{E,I}(x-\theta_{E,I})}} - \frac{1}{1+\mathrm{e}^{a_{E,I}\theta_{E,I}}}, \tag{3}$$

A_{ij} is an element of the subject-specific coupling matrix, A, whose value is the connection strength between brain regions i and j as determined from DSI data. The global strength of coupling between brain regions is tuned by excitatory and inhibitory coupling parameters c_5 and c_6 respectively. They are fixed as $c_6 = c_5/4$, representing the approximate ratio of excitatory to inhibitory coupling. $P_i(t)$ represents the external inputs to excitatory state activity and is used to perform computational stimulation experiments. The parameter τ_d^{ij} represents the communication delay between the regions i and j. If the spatial

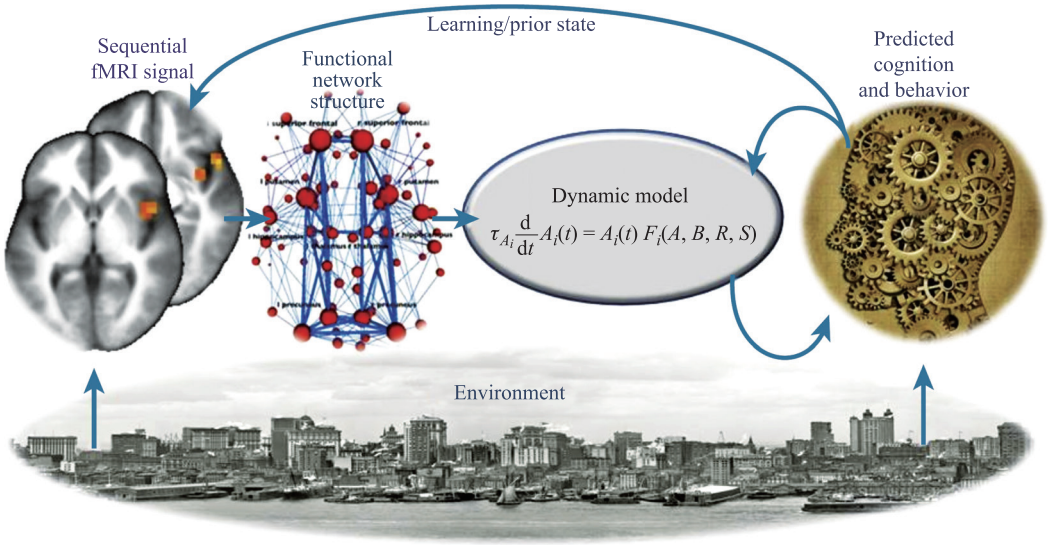

Fig. 7 Brain imaging to a low-dimensional model of cognition and behavior. Characterizing and predicting cognitive processes as measured with modern imaging techniques require the inclusion of temporal sequencing in the description of brain networks and their conceptualization as nonlinear dynamical systems. The bidirectional interaction among experimental and theoretical approaches will lead to a better understanding of the dynamics of cognitive processes. Top feedback arrow represents the influence of cognitive processes, such as learning and attention focusing, on the functional brain networks architecture. The dynamical model is represented in the general form of coupled kinetic equations for the activities $A_i(t)$ of the cognitive modes. In this representation, function F characterizes the competition of the modes that can depend on internal and external conditions represented by the parameters in parentheses. Reproduced from Ref. [43].

distance between the regions i and j is d_{ij}, $\tau_d^{ij} = d_{ij}/\tau_d$, where $\tau_d = 10$ m/s is the signal transmission velocity. Additive noise is input to the system through the parameters $w_i(t)$ and $v_i(t)$ which are derived from a normal distribution and $\sigma = 10^{-5}$. Other constants in the model are biologically derived: $c_1 = 16, c_2 = 12, c_3 = 15, c_4 = 3, a_E = 1.3, a_I = 2, \theta_E = 4, \theta_I = 3.7, \tau = 8$ as described in references [44, 45].

An important feature of the Wilson–Cowan oscillator is that an uncoupled oscillator can exhibit one of three states, depending upon the amount of external current applied to the system [45]. When no external current is applied ($P = 0$), the system relaxes to a low fixed point, see Figs. 8(a) and (b). For moderate amounts of applied current, the oscillator is pushed into an oscillatory limit cycle, and if sufficiently high amounts of current are applied, the system settles at a high fixed point.

An equivalent model is the neural mass model [46, 47], which describes the mean field activity of a neuronal population. This low-dimensional model with biological plausible interactions between excitatory and inhibitory neural populations can generate oscillations in the alpha band (~ 10 Hz) and is used to represent resting brain states [48]. There are now increasing evidences to show that the local circuits in the cortical regions are not identical [49], but display heterogeneity in neuronal density and spine density, etc. However, modeling the regions with simplified assumption of identical neural mass oscillators allow us to focus on the effect of underlying network architecture on the dynamical patterns. The dynamical equations of identical neural mass oscillators coupled by the underlying cortical network read as

$$\begin{aligned}
\ddot{v}_I^p &= Aaf(v_I^e - v_I^i) - 2a\dot{v}_I^p - a^2 v_I^p, \\
\ddot{v}_I^i &= BbC_4 f(C_3 v_I^p) - 2b\dot{v}_I^i - b^2 v_I^i, \\
\ddot{v}_I^e &= Aa[C_2 f(C_1 v_I^p) + p_I \\
&\quad + \frac{c}{\lambda_I}\sum_{J=1}^{N} M_{IJ} f(v_J^e(t-\tau) - v_I^e)] - 2a\dot{v}_I^e - a^2 v_I^e, \qquad (4)
\end{aligned}$$

where $I = 1, \cdots, N$, v_I^p, v_I^i and v_I^e are the post-synaptic membrane potentials for three subpopulations (pyramidal, inhibitory and excitatory) of the node-I, respectively. The sigmoid function $f(v)$ converts the average membrane potential into an average pulse density of action potentials, which propagate among subpopulations within each node and between nodes through synaptic coupling. The parameters A and B represent the average synaptic gains, $1/a$ and $1/b$ are the average dendritic-membrane time constants. C_1 and C_2, C_3 and C_4 are the average number of synaptic contacts among the subpopulations. M_{IJ} is the coupling matrix with the real connection weights from the data of Refs. [18, 20]. The coupling strength c is normalized by the mean intensity λ_I across the nodes, where $\lambda_I = \sum_J^N M_{IJ}$ is the total input weight to node-I. τ is the time-delay for interregional signal transmission, assumed to be common for different links.

In numerical simulations, both the coupling matrix A_{ij}

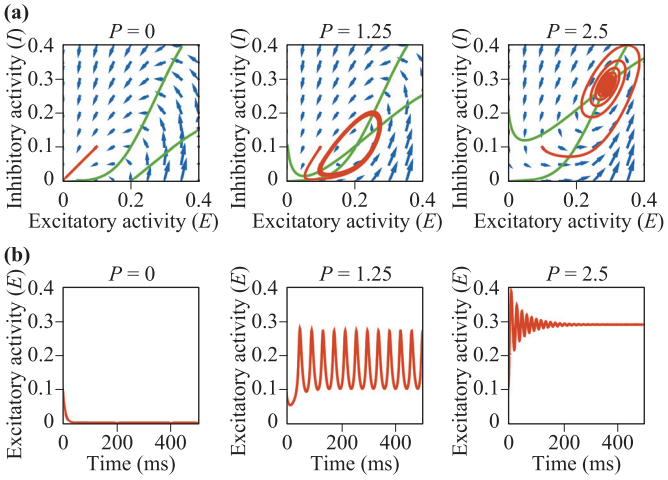

Fig. 8 Nonlinear brain dynamics and variability. **(a)** Excitatory–inhibitory phase space plots depicting behavior for a single Wilson–Cowan oscillator in the presence of no external current input (left; $P = 0$; low-fixed point), moderate external current input (middle; $P = 1.25$; limit cycle), and high external current input (right; $P = 2.5$; high fixed point). All simulations are started with initial conditions $E = 0.1, I = 0.1$ and nullclines are plotted in green. **(b)** The corresponding firing activities of the excitatory population plotted as a function of time for the simulations depicted in (a). Reproduced from Ref. [45].

of Eq. (2) and M_{IJ} of Eq. (4) can be chosen from the resting-state. Recent evidence suggests that resting-state functional network reflects the human brain's invariant global routing architecture. Supporting this, it has been demonstrated that most of the functional network topology variance present during task performance (80%) is already present during rest. Thus, resting-state functional connectivity primarily reflects an intrinsic functional network architecture that is present regardless of cognitive context, given that there are only moderate changes to functional network organization across tasks [50].

5 Current progress in the mechanisms of brain functions

Experiments have shown that cortical networks exhibit diverse patterns of activity, such as oscillations, synchrony, and waves. During neuronal activity, each neuron can receive inputs by thousands of other neurons and, when it reaches a threshold, redistributes this integrated activity back to the neuronal network. So far, how to scientifically analyze the massive and high-dimensional brain data has become a new challenge for researchers. In recent years, complex network analysis has been successfully applied to the study of brain science and formed a new branch of brain science, i.e., brain connectome, which has now become one of the most active research fields.

Up to now, the studying of brain network has discovered a variety of important mechanisms of brain functions such as the small world effect, community topology, and hierarchical and rich-club connectivity. However, there are still many important open problems which are waiting for us to solve. For simplicity, we here classify them into three aspects: (i) The first aspect is how the consciousness emerges from a population of neurons. This problem has been studied for a long time and a general idea is the emergence of synchronization. Currently, its study is focused on partial synchronization such as the chimera states and spatiotemporal chimera states. The derived problem is the continuous and discontinuous phase synchronization, i.e., the first and second phase synchronization. The unclear problem is the switching between the first and second phase synchronization and their coexistence, etc. (ii) The second aspect is about the functional integration and segregation. It is well known that the organization of the human brain is governed by two fundamental principles: functional integration into large-scale networks, which is realized through long-range connections, and functional segregation into distinct regions, which is realized through local differentiation. Importantly, these two principles are not mutually exclusive but rather jointly form the neurobiological basis of all higher brain functions that arise from interactions between specialized regions. The question is how to implement the functional integration and segregation in brain networks by dynamical models. In this way, we may understand the mechanism of the unification of the two principles. Currently, its study is focused on clustering synchronization [51]. The untouched problem is the topic of multiple stimulated signals and the mutual influence between the activated subnetworks of cognitive function and the inactivated subnetworks of background. (iii) The third aspect is how the functional network comes from the structural network. As pointed out in Section 3, the functional brain network is distinct from the structural brain network but generated from it. A general approach to measure the functional brain network is through the Pearson correlation coefficient of measured time series. But this approach does not tell us where the correlation comes from. To figure out the answer, its current study is focused on the research directions of remote synchronization and remote propagation. They are hopeful directions but still long way to go.

In sum, it will be not easy to figure out all the answers for these three aspects, even part of them. Fortunately, some progresses have been achieved so far, with the help of complex network analysis. We here make a brief discussion on these achievements as follows.

5.1 Chimera states in brain networks

A paradigmatic example to study the mechanisms of brain functions is the effect of unihemispheric sleep, which has been observed in some birds and aquatic mammals (Cetaceans, eared seals and manatees) and in numerous lizards, turtles and tortoises, and caiman. In unihemi-

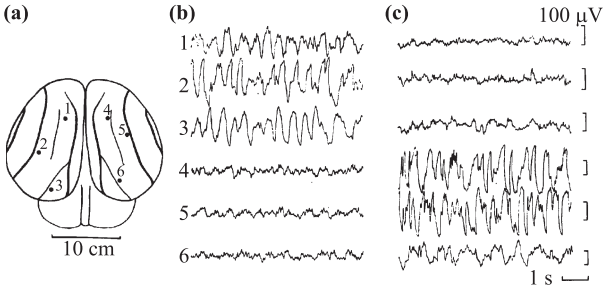

Fig. 9 EEG recorded from the parieto-occipital cortex **(a)** of a bottlenose dolphin during unihemispheric slow-wave sleep with either the left **(b)** or right **(c)** hemisphere asleep. Note the high-amplitude, low-frequency EEG activity in the sleeping hemisphere and the low-amplitude, high-frequency EEG activity in the awake hemisphere. Reproduced from Ref. [54].

spheric sleep, brain activity measured by EEG shows a pattern characteristic of sleep in one hemisphere, while the other hemisphere shows brain waves more closely resembling wake related activity, i.e., with one cerebral hemisphere sleeps while the other remains awake [52]. It was even interestingly reported that ducks arranged in a row sleep largely bihemispherically when safely flanked by others, yet switch to sleeping unihemispherically when on the edge of the group, and orient their open eye away from the others as if watching for potential threats [53]. To see it more details, Fig. 9 shows the time series of such an example, where (a) represents the positions of electrodes, and (b) and (c) show the EEG recorded from the parieto-occipital cortex of a bottlenose dolphin during unihemispheric for slow-wave sleep with either the left (b) or right (c) hemisphere asleep [54]. Obviously, in either (b) or (c), the time series of electrodes $1-3$ are different from that of electrodes $4-6$, marking the unihemispheric sleep. Moreover, the difference between (b) and (c) manifests the switching of sleep between the two hemispheres.

It was assumed that the reason for unihemispheric sleep is to mitigate the fundamental conflict between sleep and wakefulness as reduced vigilance is the conspicuous cost of sleep in most animals. According to this assumption, our human being should also have unihemispheric sleep when we are in an unsafe night. However, this scenario had not been confirmed until 2006 that Tamaki *et al.* [55] found that when humans sleep in a novel environment, the default-mode network in one hemisphere is kept more vigilant to wake the sleeper up as a night watch upon detection of deviant stimuli, which is called the *first-night effect* (FNE) in human sleep.

To study the physics mechanism of unihemispheric sleep, Abrams and Strogatz [56] presented a coupled oscillators model to implement the coexistence of one completely synchronized part and another completely desynchronized part in 2004 and named it as chimera state. The difficulty of this coexistence is that all the coupled oscillators are identical and their stable attractor is the synchronization solution, thus the state of coexistence is unstable and is generally unobservable. After that, numerous efforts have been paid to this topic, such as the neuron systems, experimental systems, and multiple chimera states, see reviews [57–60] for details. However, most of these works are only focused on the mechanisms or conditions of chimera states but have no direct relationship with real brain networks. Moreover, a few works have discussed the alternating activity patterns between the hemispheres over time [61], i.e., the switching phenomenon of Fig. 9, and extension to complex networks [62]. Recently, some attention has been paid to the case of real brain networks [63, 64]. We here discuss three of these works that are closely related to the real brain networks.

The first one is contributed by Bansal *et al.* [8] in 2019. This work considered an empirical brain network consisting of 76 brain regions (or nodes) and paid attention to how brain structure influences the dynamical patterns produced by stimulation. They divided this network into nine cognitive systems by using personalized brain network models, where each of them consists of the coactivated regions for supporting a generalized class of cognitive functions. Then, they presented a chimera-based, cognitively informed framework to study how large-scale brain structure influences brain dynamics and functions. They found that all nine systems produce chimera states due to stimulations and named them cognitive chimera states.

The second one is contributed by Kang *et al.* [65] in 2019. They considered the empirical brain network of Fig. 4 with 989 nodes and considered it as a two-layered network with the left and right hemispheres of cerebral cortex being different layers, respectively. In this model, the intra-coupling strength λ_{in} and inter-coupling strength λ_{out} are considered to be different. They found that the model can reproduce a variety of different dynamical behaviors, including the phenomenon of unihemispheric sleep. Figure 10 shows the results for four typical cases where ω_i^r and ω_i^l are the effective frequencies of the oscillator i in the right and left hemispheres, respectively, and the insets are their corresponding dynamics, i.e., u_i^r and u_i^l, respectively. From Fig. 10 we see that (a, e) represent the case of disorder in both hemispheres; (b, f) the case of chimera state in both hemispheres; (c, g) the case of disorder in the right hemisphere but synchronization in the left hemisphere, indicating the case of unihemispheric sleep; and (d, h) the case of synchronization in both hemispheres. In sum, the first case of Figs. 10(a) and (e) and the last case of Figs. 10(d) and (h) denote the two extreme states of desynchronized and synchronized states, respectively. The second case of Figs. 10(b) and (f) represents a chimera state where there is a plateau of ω_i in both the up and down panels and their insets show a coexistence of synchronized and unsynchronized $u_i(t)$. The most interesting is the third case of Figs. 10(c) and (g) where the right hemisphere is disordered but the left hemisphere is

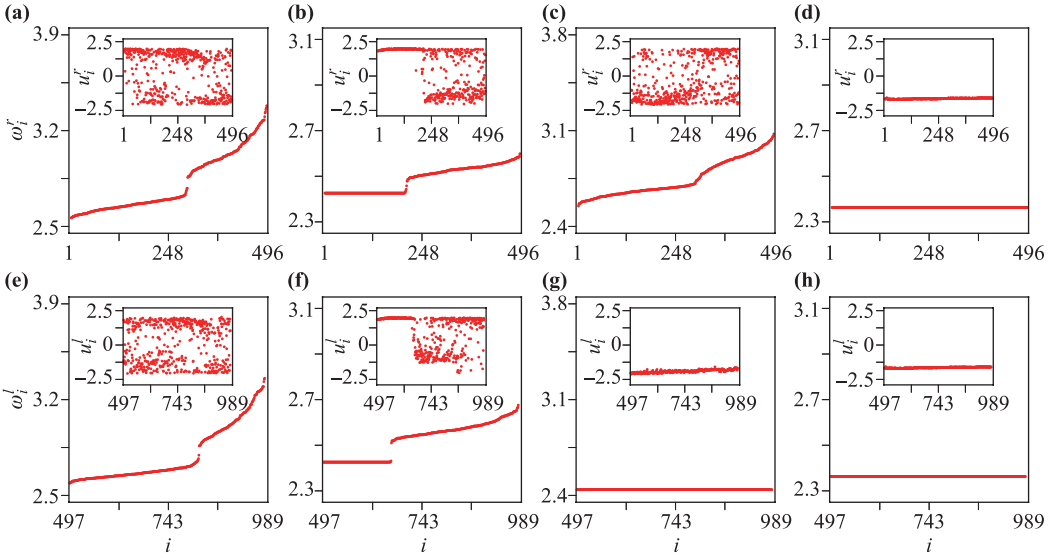

Fig. 10 Four typical dynamical states in the two-layered brain network model where the upper panels represent the right hemisphere and down panels the left hemisphere. The inset in each panel is a snapshot of u_i at time t. **(a)** and **(e)** represent the case of disorder with $\lambda_{in} = 0.1$ and $\lambda_{out} = 0.3$; **(b)** and **(f)** the case of chimera state with $\lambda_{in} = 0.1$ and $\lambda_{out} = 1.8$; **(c)** and **(g)** the case of unihemispheric sleep with $\lambda_{in} = 0.4$ and $\lambda_{out} = 3.5$; and **(d)** and **(h)** the case of synchronization with $\lambda_{in} = 4.0$ and $\lambda_{out} = 3.5$. Reproduced from Ref. [65].

synchronized, marking the unihemispheric sleep.

The third one is contributed by Huo *et al.* [66] in 2021. They also considered the empirical brain network of Fig. 4 with 989 nodes but focus on how to produce the diversity of patterns. More precisely, they let each node be represented by the mean-field mass model of Eq. (4). Except the collective behaviors of global network, Huo *et al.* also considered the local behaviors of brain network. As pointed out in Fig. 4, this brain network can be parcellated into 64 functional regions and each one contains N_j nodes, with $\sum_{j=1}^{64} N_j = 989 = N$. To quantify and distinguish the patterns, an order parameter R can be adopted as follows:

$$R\mathrm{e}^{\mathrm{i}\phi} = \frac{1}{N_j}\sum_{k=1}^{N_j}\mathrm{e}^{\mathrm{i}\theta_k}, \tag{5}$$

where R characterizes phase coherence, ϕ the average phase, θ the phase of oscillator, and N_j the number of coupled oscillators to be examined.

By calculating the order parameter R for each of the 64 functional regions, it is revealed that the dynamics of each region typically consists of the coexistence of coherent and incoherent groups of oscillators, suggesting that chimera state also appears at the local level of functional regions. Thus, chimera state in brain network can be observed on both the global and local levels, which is called spatial multi-scaled chimera states [66]. Let the physical position of each functional region be the average of the positions of all its N_j nodes on the cerebral cortex. Figure 11(a) shows the position distribution of these 64 functional regions in human brain network where the numbers are the index of these regions and their functional names are given in Fig. 4. The original 989 nodes of Fig. 4 are remained as the gray background of Fig. 11(a), for visualization effect. For a set of specific parameters with a small R at the global level, the different colors of points in Fig. 11(a) show the values of R in the 64 functional regions. We see that the degree of synchronization differs across cortical regions in the whole brain. To confirm the feature of chimera state in local level, Figs. 11(b)–(d) shows the snapshots of those

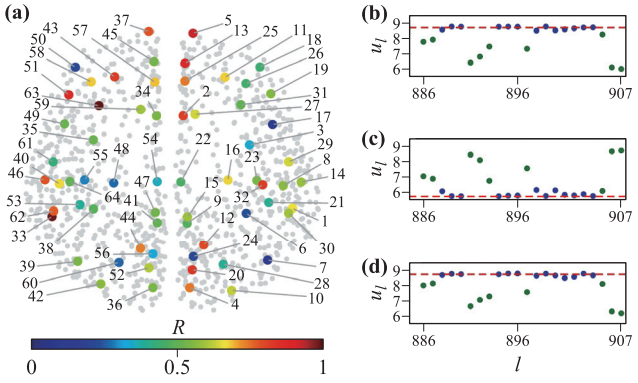

Fig. 11 Spatial multi-scaled chimera states. **(a)** Local representation of R, where the color points with numbers represent the network of the 64 local regions and the gray background points represent the network of 989 nodes. The functional names of these 64 local regions are given in Fig. 4. **(b–d)** show three arbitrary snapshots for the oscillators within the cortical region 38 from (a), respectively, where the blue oscillators on the dotted lines represent the synchronized cluster which is stable. Reproduced from Ref. [66].

oscillators within the cortical region 38 from Fig. 11(a) for three arbitrary moments, respectively. We see that the oscillators on the dotted lines represent the synchronized clusters and others unsynchronized, confirming the coexistence of stable synchronized cluster with incoherent oscillators, i.e., a chimera state within the region 38.

Ref. [66] pointed out that these patterns of spatial multi-scaled chimera states can be activated and recruited under different parameters to form diverse combinations of coherent-incoherent states. These results may help to explain the multiple brain rhythms observed in experiments.

5.2 Remote synchronization in brain networks

Except the chimera state, another hot topic of synchronization in brain network is the remote synchronization, which is characterized by the synchronization of pairs of nodes that are not directly connected via a physical link or any sequence of synchronized nodes. Remote synchronization was firstly revealed as a zero time lag synchronization among remote cerebral cortical areas by multielectrode recordings [67]. As the axonal conduction delays among distant regions can amount to several tens of milliseconds, the zero time lag synchrony among such distant neuronal ensembles must be established by mechanisms that are able to compensate for the delays involved in the neuronal communication. Its biological significance derives from the observation that such precise and coordinated spike timing correlates with perception and behavioral performance [27, 68, 69].

Remote synchronization is closely related to functional connectivity of distant cortical regions where functional correlations have also been observed between cortical regions without apparent neural links [70]. To understand the mechanisms generating functional connectivity between distant cortical regions, it has been suggested that indirect connections and collective effects governed by the network properties of the cortex play a significant role. Vuksanovic and Hovel [70] showed that remote synchrony between pairs of nodes clearly arises from symmetry in the interactions, which are quantified by the number of shared neighbors. A larger joint neighborhood positively correlates with a higher level of synchrony, i.e., a large overlapping neighborhood in complex networks of brain interactions gives rise to functional similarity between distant cortical regions. This symmetry can be defined by the size of shared neighborhoods of the synchronized nodes.

In contrast to the approach of symmetry, Bergner *et al.* [71] presented an alternative approach for remote synchronization. They studied phase synchronization in a network motif with a starlike structure in which the central node's (the hub's) frequency is strongly detuned against the other peripheral nodes. For example, for a star motif with one hub and four peripheral nodes, the frequencies can be chosen as $\omega_1 = 2.5$ for the hub node and $\{\omega_n\}_{n=2}^{5} = \{0.975, 0.992, 1.008, 1.025\}$ for the peripheral nodes, i.e., the frequency of the hub node is larger than two times of that of the peripheral nodes. They interestingly found that the peripheral nodes form a phase synchronized cluster, while the hub remains free with its own dynamics and serves just as a transmitter for the other nodes. That is, remote synchronization is induced by a transmitter.

However, the intrinsic frequencies of neurons in a specific cognitive subnetwork generally do not have so large difference and thus it is better to consider them as approximately identical oscillators. Then, an interesting question arises: whether it is possible to observe remote synchronization in the systems of identical oscillators. To answer this question, Kang *et al.* [72] considered the case of identical oscillators but did not observe the remote synchronization. Fortunately, they found that remote synchronization can be still observed, provided that a time delay is considered. This condition is reasonable as the axonal conduction delays in cerebral cortex can amount to several tens of milliseconds [67]. Kang *et al.* also considered the empirical brain network of Fig. 4 with 989 nodes and let the node dynamics be equipped with the Stuart–Landau oscillator as follows:

$$\dot{u}_j = (\alpha + \mathrm{i}\omega - |u_j|^2)u_j + \varepsilon \sum_{k=1}^{N} W_{jk}(u_k(t-\tau) - u_j(t)), \quad (6)$$

where $\mathrm{i} = \sqrt{-1}, j = 1, 2, \cdots, N = 989$, W_{jk} denotes the weighted connection matrix from [18, 20]. $\sqrt{\alpha}$ and ω are, respectively, the amplitude and natural frequency of oscillator i when uncoupled. ε is the coupling strength, and τ is the time delay.

To conveniently study the patterns of remote synchronization in the empirical brain network, Kang *et al.* [72] extracted both the hub nodes and all their synchronized leaf nodes but ignored the unsynchronized leaf nodes. In this way, they found many star motifs with remote synchronization in the empirical brain network. Figure 12

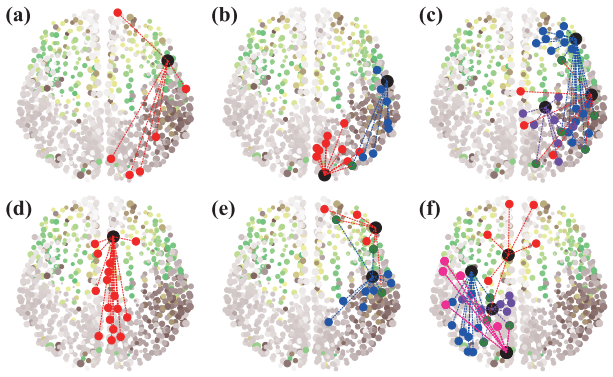

Fig. 12 Six typical patterns of remote synchronization for $\tau = 0.5$ and $\varepsilon = 0.1$. Each pattern is chosen by the conditions: (i) there is no synchronization between the hub and its peripheral nodes; and (ii) all the peripheral nodes are synchronized each other. Reproduced from Ref. [72].

shows six typical patterns of remote synchronization for $\tau = 0.5$ and $\varepsilon = 0.1$. Similar patterns of remote synchronization can be also found for other sets of parameters τ and ε in the empirical brain network. From Fig. 12 it is clear that each of the patterns in the second and third columns has two or more hub nodes, in contrast to the patterns with only one hub node in the first column. This finding may be significant as it is distinguished from the paradigmatic pattern of remote synchronization with only one hub node in previous studies.

A common feature for the patterns in the second and third columns of Fig. 12 is that two hub nodes are connected by some common leaf nodes. To understand the mechanism of these patterns of remote synchronization with two or more hub nodes, Kang *et al.* [72] presented a new framework of remote synchronization as shown in Fig. 13, where the nodes with red, blue and pink numbers represent the hub, leaf and common leaf nodes, respectively. They found that with the increase of coupling strength ε, the two leaf clusters of the hub nodes "1" and "2" will first self-synchronize at ε_{c1}, respectively, but do not synchronized each other, and then the two synchronized leaf clusters will gradually merge into a larger synchronized one at $\varepsilon \approx \varepsilon_{c2}$ [72]. In this process, the common leaf nodes "8" and "9" do take a key role for remote synchronization in the framework of Fig. 13. This result shows a new way for remote synchronization to appear in different local places of cerebral cortex and thus may be helpful to understand the functional connectivity of distant cortical regions.

5.3 Explosive synchronization in brain networks

Another approach to understand brain functions is through pathological disorders such as the epileptic seizure. In general, epilepsy has four phases: the interictal period, the onset of the seizure, and the propagation and termination phases. It is found that the coupling between brain areas during seizures changes with time, increasing or decreasing at the seizure onset in different cases [73]. Both the onset and termination processes are

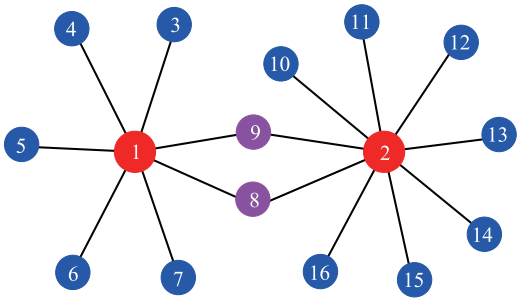

Fig. 13 A schematic figure of the new framework of remote synchronization with two hubs, where the nodes with red, blue and pink numbers represent the hub, leaf and common leaf nodes, respectively. Reproduced from Ref. [72].

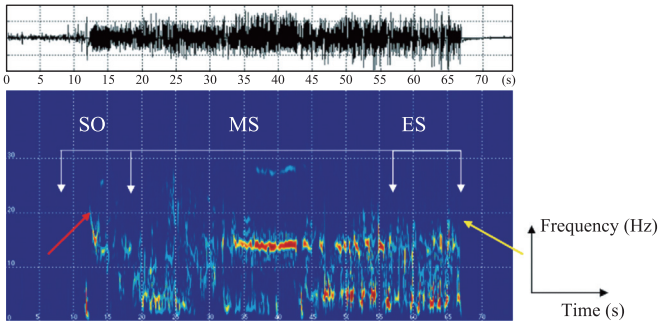

Fig. 14 Definition of the time-frequency (TF) representation of a seizure recorded in the Hip from a patient with mesial TLE (Temporal lobe epilepsy). TF is used to reveal the high-frequency activity at the seizure onset (red arrow) and the end of rhythmic ictal activity (yellow arrow) recorded here in the Hip. The period SO (seizure onset) includes 5 s before and 5 s after the onset of high-frequency activity. The period ES (end of seizure) is defined as the last 10 s of the seizure. Period MS (middle of seizure) is the junction between these two periods. Reproduced from Ref. [74].

very fast, indicating a jumping phase transition at critical coupling. Fig. 14 shows such as an example of temporal lobe epilepsy [74]. It is clear that both the SO (seizure onset) and ES (end of seizure) are suddenly happened.

Figure 14 reveals that during the seizure, synchronization is significantly higher than that of the background period, indicating a jumping transition called as explosive synchronization. Wang *et al.* [75] analyzed intracranial electroencephalography (IEEG) recordings of a seizure episode from a epilepsy patient and uncovered that explosive synchronization-like transition occurs around the clinically defined onset of seizure. This phenomenon recently got much attention in the field of complex networks and many different models have been presented to describe its mechanisms [76–83]. A characteristic feature of explosive synchronization is that its forward and backward processes are different and thus form a hysteresis loop. Therefore, two key elements of explosive synchronization are the jumping transition and hysteresis loop.

On the other hand, the explosive synchronization with a hysteresis loop has also been observed in the brain during anesthetic state transitions [84–86]. Anesthetics is very popular for humans by which an annual 234 million surgical procedures are performed worldwide. During the process of anesthetics, a patient will undergo two stages, i.e., gradually become unconscious and then re-establish consciousness upon emergence from anesthesia. One common belief is that emergence from anesthesia is the inverse process of induction. However, these two stages are of significant difference and thus make the inhaled general anesthetics offer the opportunity to study the molecular and neuroanatomical pathways essential for the aroused, conscious state as well as the orderly transition to and from the unconscious state. These two stages may have the same mechanism with the alternating activity between

states of conscious wakefulness and the unconsciousness associated with natural sleep. As with wake and sleep, consciousness and anesthetic-induced unconsciousness are bistable, as subjects exist in only one of the mutually exclusive states at a time.

Experimentally, Friedman *et al.* [85, 86] studied anesthetic-induced unconsciousness and wakefulness in both mice and fruit flies and found that different concentrations of anesthetics are required for induction of and emergence from general anesthesia. Take the mice as an example. By definition, anesthetic induction in mice occurs at the drug concentration at which the righting reflex is lost, whereas emergence occurs at the concentration at which the righting reflex returns. Figure 15 shows the results of wild-type mice exposed to volatile anesthetics where (a) and (b) represent the cases of halothane dose-response and isoflurane dose-response, respectively. We see that both (a) and (b) exhibit hysteresis between induction and emergence but there is a jumping transition in (a) but no jumping transition in (b). A more comprehensive description is shown graphically by the shaded area bracketed between the solid induction and dashed emergence curves.

Instead of the case of animals, Kim *et al.* [87] studied the case of humans and focused on the functional and topological conditions for explosive synchronization developed in human brain networks with the onset of anesthetic-induced unconsciousness. For human beings, the mechanisms of the emergence from unconsciousness in sleep, anesthesia, and coma are still elusive, although they share a number of neural features but the recovery profiles are radically different. Thus, the studying of anesthetic-induced unconsciousness is also a good window for understanding the mechanism of brain functions. During anesthetics, diverse anesthetics reduce network communication and the capacity of information integration, which is thought to be necessary for consciousness. In the experiment, Kim *et al.* [87] constructed the functional brain networks from multi-channel EEG recordings in seven healthy subjects across conscious, unconscious, and recovery states. They demonstrated for the first time that the network conditions for explosive synchronization, formerly shown in generic networks only, are present in empirically-derived functional brain networks.

Kim *et al.* [87] used the inhaled anesthetic sevoflurane to gradually modulate the level of consciousness across multiple states: eyes-closed waking, unconsciousness, recovery, and the transitions between. They found that slow titration of the inhaled anesthetic sevoflurane results in a dose-dependent reconfiguration of network topology and dynamics. Figure 16 shows the results for two volunteers whose recovery trajectories represent gradual and abrupt state transitions to responsiveness, respectively. Figure 16(a) shows the case of slow loss and recovery of responsiveness. In order to show a trend of temporal change, the responsiveness was smoothed by averaging 5 min long time window and moving it 30 s. It took about 40 min for the subject in Fig. 16(a) to reach the point of 0% responsiveness (from 20 to 60 min in Fig. 16(a), black line), and 25 min to recover back to 100% responsiveness (from 65 to 90 min). While Fig. 16(b) shows fast loss and recovery of responsiveness. The participant first lost responsiveness around 10 min in Fig. 16(b); the time taken for loss and recovery of 100% responsiveness were about 5 min. Correlating this with a change of network properties, the two subjects demonstrated dramatically distinct patterns of suppression strength S, which represents a suppressive anesthetic effect on local synchronization [87]. That is, Fig. 16(a) demonstrates gradual changes of S, while Fig. 16(b) shows an abrupt increase of S before the first large drop of responsiveness and then maintains large S during the anesthetized state.

5.4 Intelligence quotients from brain networks

It is well known that in our society, some people are smart while others are not. In particular, a specific person may be smart at gaining knowledge but not smart at master-

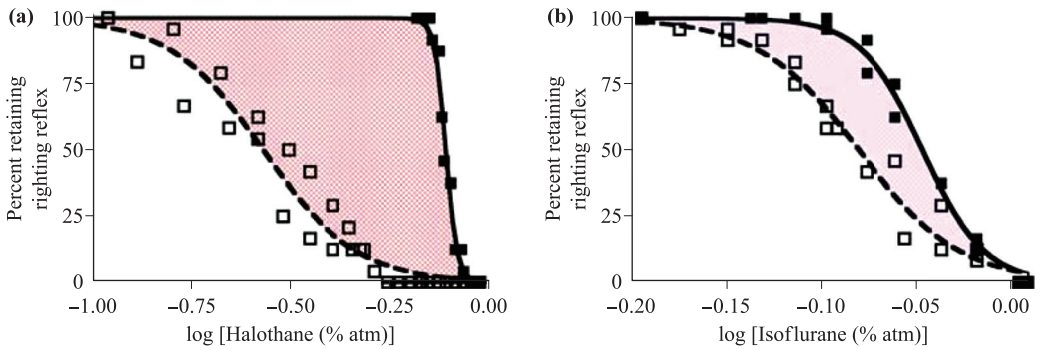

Fig. 15 Neural inertia in wild type mice. Within the shaded area, subjects will be awake or anesthetized depending upon their previous state of arousal. This area represents a resistance to change in arousal state and graphically depicts neural inertia. **(a)** Halothane dose-response curve in wild-type mice for induction and emergence. **(b)** Isoflurane dose-response in wild-type mice. Reproduced from Ref. [85].

ing skills. The measure most commonly used to quantify smartness is that of intelligence, often termed the intelligence quotient (IQ). Undoubtedly, IQ is close to the topology of brain network and has always been an efficient way to study brain functions. From the very beginning of intelligence research, there has been a profound interest in linking inter-individual differences measured by psychometric test instruments to differences possessing a neurobiological substrate. It was usually assumed that individuals with more cortical brain volume possess more neurons and thus exhibit more computational capacity during reasoning.

However, modern techniques such as MRI have revealed that intelligence is not a function of how hard the brain works but rather how efficiently it works, an observation known as the neural efficiency hypothesis of intelligence [88]. In addition, neuroimaging studies have shown that intelligent individuals, despite their larger brains, tend to exhibit lower rates of brain activity during reasoning. By combining advanced multi-shell diffusion tensor imaging with a culture-fair matrix-reasoning test, Genc *et al.* found that higher intelligence in healthy individuals is related to lower values of dendritic density and arborization [89]. That is, the neuronal circuitry associated with higher intelligence is organized in a sparse and efficient manner, fostering more directed information processing and less cortical activity during reasoning. Figure 17 shows the results.

On the other hand, we also know that the brain consumes about 20% of the body's energy although it is only about 2% of the body weight. Thus, the brain network has to be a trade-off between minimizing energy consumption and maximizing efficiency. Two obvious but apparently contradictory constraints are low wiring cost and high processing efficiency, characterized by short overall wiring length and a small average number of processing steps, respectively. Growing evidence shows that neural networks are results from a trade-off between physical cost and functional value of the topology. To explain this trade-off, Chen *et al.* [90] presented an approach to quantitatively measure this trade-off in the networks of Macaque cortical connectivity and *C. elegans* neuronal connections. This approach is based on the fact that the wiring of the whole neural network of the Macaque cortex and *C. elegans* neuronal network are optimized under the single wiring cost constraint- the total wiring could be decreased to 64% of the original length in Macaque and to 52% in *C. elegans* [91] when applying the component placement optimization to minimize the total wiring length while preserving the specific network connectivity. Alternatively, it has been suggested that constraints such as signal propagation efficiency, measured by the global minimization of processing steps across the network, may shape the organization of neural systems [92]. In conclusion, these two constraints need to be considered in combination. For this purpose, Chen *et al.* [90] used the total physical distance of the wiring L_p to represent the effect of the wiring cost constraint, and the total graph distance of the shortest paths L_g to represent the influence of the processing efficiency constraint, and defined an objective function L as a combination of both constraints using a weight parameter α, namely,

$$L = (1-\alpha)L_g + \alpha L_p, \tag{7}$$

with L_g and L_p appropriately normalized. So $\alpha = 0$ or

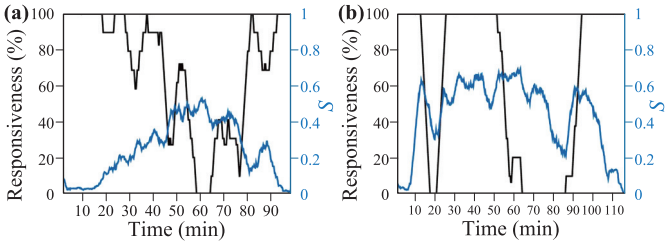

Fig. 16 Two representative subjects for gradual and abrupt state transitions. The responsiveness (black line) and suppression strength S (blue line) of **(a)** the gradual and **(b)** abrupt state transition are presented. The responsiveness was averaged by 5 min time period with shifting 30 s to show the trend of temporal change. In comparing the two subjects, the gradual state transition has a lower S, whereas the abrupt state transition has a relatively higher S. Reproduced from Ref. [87].

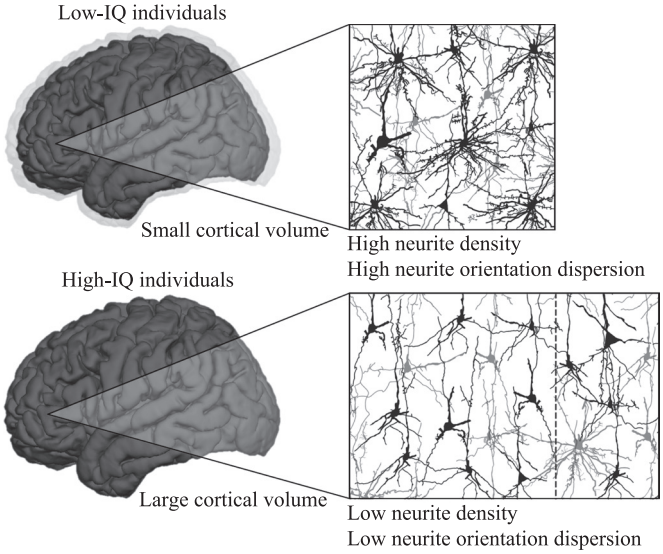

Fig. 17 Schematic depiction of differences between low-IQ and high-IQ individuals with regard to brain volume, neurite density, and arborization of dendritic trees within the cortex. High-IQ individuals are likely to possess more cortical volume than low-IQ individuals, which is indicated by differently sized brains (left side) and differently sized panels showing exemplary magnifications of neuron and neurite microstructure (right side). Due to their larger cortices, it is conceivable that high-IQ individuals benefit from the processing power of additional neurons, which are marked by the dotted line in the lower panel. Reproduced from Ref. [89].

$\alpha = 1$ corresponds to a single constraint of path efficiency or wiring cost, respectively. By Eq. (7), an optimal α can be figured out for the minimum of L, i.e., the solution of trade-off.

Chen's approach of index α did not discuss the aspect of IQ as their data are from animals [90]. To extend this approach to the case of humans, the aspect of IQ has to be considered. For example, it was revealed that the values of IQ for females are statistically different from that for males. In general, males score higher on the spatial navigation problems, mental rotation test, embedded figures test, and engineering and physics problems, whereas females perform better on emotion recognition, verbal fluency, and social sensitivity [93]. Increasing evidence has also shown that IQ depends not only on the aspect of phenomenology such as the size of brain and sexuality but also on the topology of the brain network [94]. To figure out the relationship between the trade-off and IQ, Cao *et al.* [95] recently focused on the real data of 63 subjects with known IQ and constructed their brain networks from the data. They interestingly found that IQ has a positive correlation with the total wiring length of the links l_p and a negative correlation with the processing efficiency l_g. Thus, they modified Eq. (7) into

$$L = (1-\alpha)\frac{l_g - l_g^{min}}{l_g^{max} - l_g^{min}} + \alpha\frac{l_p - l_p^{min}}{l_p^{max} - l_p^{min}}, \tag{8}$$

so that both the two terms of Eq. (8) may change from 0 to 1, where l_p^{max} corresponds to the case of $\alpha = 1$ and l_g^{max} corresponds to the case of $\alpha = 0$. Similar to Eq. (7), an optimal α can be figured out by Eq. (8) for the minimum of L, which represents the trade-off between wiring cost and processing efficiency. Cao *et al.* [95] calculated the optimal α for each subject from the real data of the cerebral cortex and found that the correlation between optimal index α and IQ is negative but females have a stronger correlation than males. This is consistent with the established sex differences showing better spatial abilities in males and better verbal abilities in females [94].

To further find out the mechanism for the functional difference between males and females, Cao *et al.* [95] considered the local level of brain regions and studied the relationship between regional optimal α and IQ. They calculated the Pearson coefficient $r(X, Y)$ by Eq. (1), where X represents the full IQ, verbal IQ, and performance IQ, respectively, and Y represents l_p and l_g, respectively. Let r_m and r_f be the Pearson coefficients for male subjects and female subjects, respectively. It is found that r_m and r_f are significantly different in some regions but similar in others. Figure 18 shows the results where all the r_m are negative but r_f can be either positive or negative. These findings show that the functional differences between individuals, including the differences between males and females, are closely related to the different running modes of their brain networks.

5.5 Remote propagation in brain networks

Except the above aspects, one more aspect to understand brain functions is the signal propagation. It is well known that in executing a normal brain function, each neuron receives electrical signals via its treelike dendrites, connected via synaptic inputs from other neurons. In this process, part of network nodes will be activated and thus form a functional brain subnetwork when a stimulus is received. Thus, a variety of functional subnetworks can be formed for different stimuli, which are associated with specific cognitive networks such as the visual networks, sensorimotor networks, auditory networks, default mode networks (DMNs), executive control networks, and some others. It is revealed that each of these functional subnetworks consists of nodes distributed in different regions, including distant nodes. Then, a key question arises: how these distant connections emerge during the formation of a specific functional subnetwork. To figure out the answer, much attention has been paid to how brain functions emerge from external stimuli or how different cognitive subnetworks are activated to respond to different external stimuli. For example, Wang *et al.* [96] studied how signals are transmitted along a chain of Rossler oscillators by frequency-locking. Liu [97] studied how an external signal is transmitted in a hierarchical organization network by introducing a self-tuning mechanism of transmission links. Bansal *et al.* [8] studied how regional brain stimulation generates different patterns of synchronization across predefined cognitive systems. These studies revealed the possibilities of signal transmission on different network topologies but did not answer how the local structures of the network influence signal propagation, especially the unique topology of the brain network with the properties of small world, richer-club, and community, etc. This problem is not trivial as its study may also help us diagnose and control diseases. For example, the treatment of an epileptic seizure is to stop the fast spread of abnormal synchronization in the brain network.

Toward this aim, Shen *et al.* [98] recently considered the neural network of *C. elegans* with 277 nodes and 2105 directional links and found an interesting effect of *remote firing propagation* between two distant and indirectly connected nodes with the intermediate nodes being inactivated. This finding is of interesting as it is in contrast to the general believing that a specific firing in a brain network may be gradually propagated from a source node to its neighbors and then to the next nearest neighbors and so on. On the other hand, this finding also implies that it is possible for the distant connections to show up by the way of remote signal propagation, which provides a possible way for functional subnetworks to emerge.

In Ref. [98], one node is initially chosen as the signal source node and all the other nodes as the target nodes. Then, it is revealed that except the normal propagation, there is an abnormal phenomenon, i.e., remote propagation between distant nodes without the activation of inter-

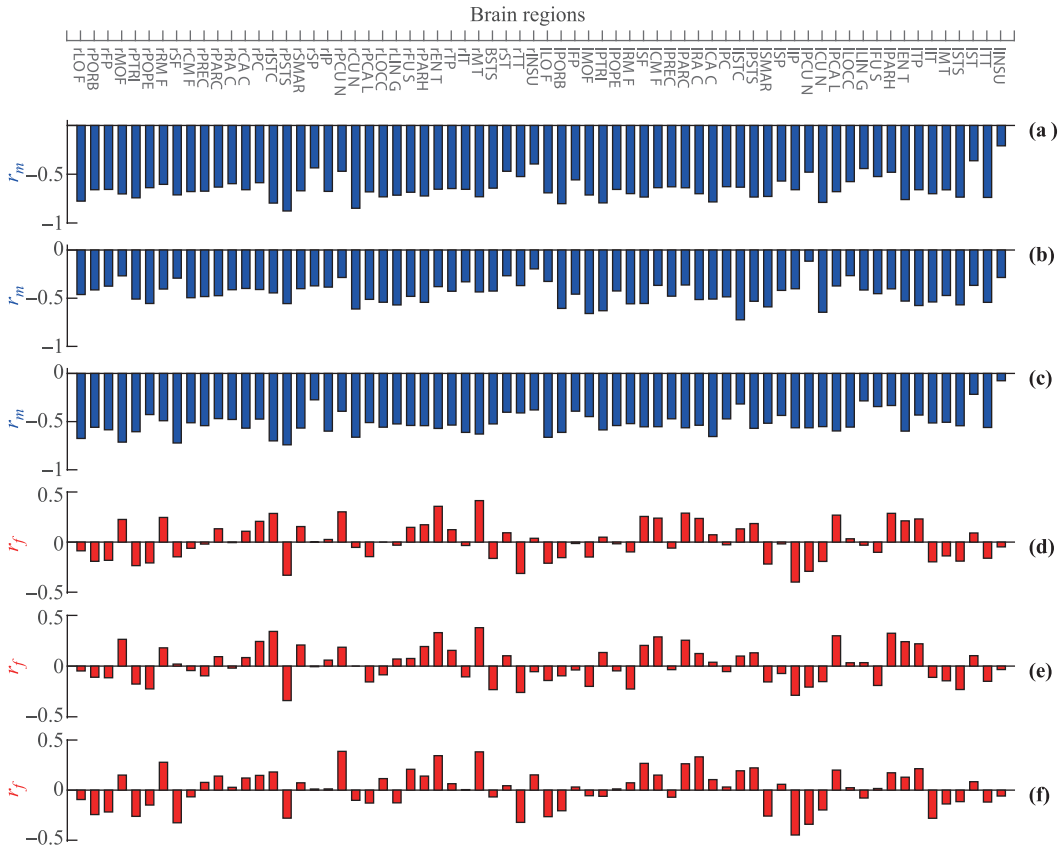

Fig. 18 Distribution of the values of r_f and r_m on different brain regions. The first row is the abbreviated names of all the 68 regions. **(a–c)** represent the case of males with (a) full IQ, (b) verbal IQ, and (c) performance IQ. **(d–f)** represent the case of females with (d) full IQ, (e) verbal IQ, and (f) performance IQ. Reproduced from Ref. [95].

mediate nodes. Figure 19(a) shows such an example of the source node 138 where the network topology is plotted as the center for the source node, the first circle for the nearest neighboring nodes of the source node, and the second circle for the next nearest neighbors and so on. The red nodes represent all the activated nodes from the source node. To make the pathway of firing propagation clear, Fig. 19(a) is simplified into Fig. 19(b) by keeping only the red nodes and those links among them, i.e., remove all the other nodes and their links. We see that only the three nodes 139–141 of the first circle are connected to source node 138 and thus form a core cluster of four connected nodes, while all the other nodes are not directly connected to them, indicating that they must be indirectly connected to the core cluster. Moreover, some of them even have no connections to others such as the nodes 46, 35, and 253, implying that they are isolated to all the other activated nodes.

Wang *et al.* [99] considered the empirical brain network of Fig. 4 and found that the effect of remote propagation can be also observed. To understand the mechanism of this phenomenon, they rechecked the nodes with remote propagation and found a characteristic feature that each node of remote propagation is connected to multiple unsuccessful propagated nodes, i.e., weak input signals from multiple channels. Thus, they simplified the brain network into a heterogeneous chain, see the schematic Fig. 20

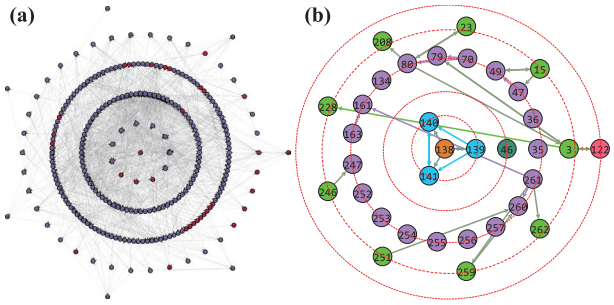

Fig. 19 A typical example of remote firing propagation where the source node is chosen as node 138. **(a)** The paths of firing propagation in the neural network of *C. elegans* where the central red node is source node 138, other red nodes are the propagated nodes, and the different circles from the center represent the nearest neighboring nodes, the next nearest neighbors, and so on. **(b)** A part of the network of (a) with only the firing nodes and the links among them, where the colors of nodes are changed to be different from circle to circle, as a guide for the eyes. Reproduced from Ref. [98].

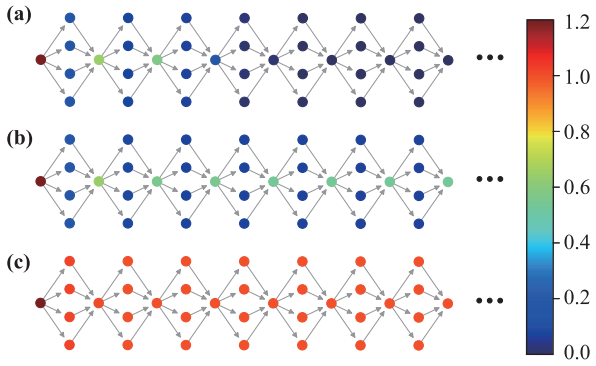

Fig. 20 Signal propagation of three typical cases for the heterogeneous chain model where (a)-(c) represent the results of finite propagation, remote propagation, and infinite propagation, respectively, with $\lambda = 0.19, 0.2$, and 0.3, respectively. Reproduced from Ref. [99].

where a hub node is directionally connected to 4 target nodes and then the 4 nodes will be directionally converged to a common hub node and so on. They found that this chain model can show different behaviors, depending on the coupling strength λ. Figure 20 shows the results where (a)–(c) represent the cases of finite propagation, remote propagation, and infinite propagation, respectively. Especially, Fig. 20(b) shows that all the hub nodes are "firing," while all the leaf nodes are not propagated, confirming the effect of remote propagation. Therefore, the accumulation of weak signals from multiple channels makes a strong input signal to the next node, resulting in remote propagation.

6 Discussion and outlook

We have systematically discussed our current understanding on brain functions from the angle of synchronization and complex network, including the aspects of structural and functional networks, methods to study brain functions, and the mechanisms of brain functions obtained so far from different partial synchronization and signal propagation. These achievements make us a fundamental step toward understanding the brain and its functions, resulting in the brain not so "black" again. However, they are still in the primary stages and far from complete understanding. First of all, the studies in Section 5.2–5.5 are all on the global level of brain network, but in fact, all the brain functions are performed on the local level of cognitive subnetworks, implying that all the related results are only a good beginning in these directions. Second, even for the relatively well studied chimera state, i.e., Section 5.1, its results are all based on the resting-state networks. It is well known that brain network dynamically changes in task-states and is thus different from the resting-state networks, although the latter are a pivotal element for understanding the dynamics and organization of the brain basal activity in health. Thus, it is also necessary to make the research of chimera state to go deeper, at least in the direction of task-states. Therefore, we still face a lot of problems. Limited by our knowledge, we suggest the following directions for future studies.

(i) Resting-state networks emerge from the correlation in signal fluctuations across brain regions during the resting state and have rich and complex dynamics, it will still be the main networks in open fields of brain networks such as the memory related fields. Especially, different resting-state networks have been associated with specific cognitive networks [100], thus the focus of partial synchronization and signal propagation should be concentrated on these subnetworks in the future studies.

(ii) Resting-state networks are also useful in detecting diseases, as they are particularly relevant to the disease-driven changes in functional connectivity. When a disease progresses, resting-state networks are in turn affected and accompanied by a loss of functional correlation between them [101]. That is, altered functional activity induced by a local dysfunction might influence the functioning of additional brain regions, leading to the spread of changes in the whole-brain functional connectivity pattern [102]. Deeper studies of this direction are needed.

(iii) Synchronization in different frequency bands may correspond to different networks and different cognitive functions [103], which will provide useful information for the mechanism of multiple rhythms of brain networks. The question how these highly structured and robust patterns of correlated activity arise from the underlying neural dynamics and structural connections still remains poorly understood.

(iv) Although functional properties are expressed locally, they are the result of the action of the entire network as an integrated system. Of course, structural connectivity places constraints on which functional interactions occur in the network [104]. An interesting question is how functional connections are predicted by structural connections. A primary step for this question is the approach of intrinsic eigenmodes [105], but further studies are definitely necessary.

(v) Our brains usually perceive signals from different senses (like touch, sound, vision) and then combine them to produce a neural response and eventually a behavioral one. In contrast to single stimulus in previous studies, this is in fact a multisensory integration and thus arises a lot of questions such as how the multi-sensory stimuli influence the remote propagation and how the multi-sensory stimuli provide a benefit to working memory processing.

In sum, the so far obtained results are great progress in understanding the brain functions and will be also the basis for future studies in these directions. Especially, the revealed brain networks (including both the structural and functional brain networks) and research approaches will be still useful for further studies. Therefore, we believe that with the increasing of data from EEG, MEG and fMRI techniques *etc*, the data-driven synchronization and complex network analysis will continuously provide new

insights to understand the mechanisms of brain functions.

Acknowledgements This work was partially supported by the National Natural Science Foundation of China under Grant Nos. 11835003, 82161148012, and 12175070, and the "Technology Innovation 2030-major Projects" on brain science and brain-like computing of the Ministry of Science & Tecknology of China (No. 2021ZD0202600).

References

1. G. Buzsaki, Rhythms of the Brain, Oxford University Press, New York, 2006
2. P. Bak, How Nature Works: The Science of Self-Organized Criticality, Springer, New York, 1996
3. L. de Arcangelis, C. Perrone-Capano, and H. J. Herrmann, Self-organized criticality model for brain plasticity, *Phys. Rev. Lett.* 96(2), 028107 (2006)
4. T. K. Hensch, Critical period regulation, *Annu. Rev. Neurosci.* 27(1), 549 (2004)
5. L. F. Abbott and S. B. Nelson, Synaptic plasticity: Taming the beast, *Nat. Neurosci.* 3(S11), 1178 (2000)
6. D. O. Hebb, The Organization of Behavior, John Wiley, New York, 1949
7. S. J. Cooper, Hebb's synapse and learning rule: A history and commentary, *Neurosci. Biobehav. Rev.* 28(8), 851 (2005)
8. K. Bansal, J. O. Garcia, S. H. Tompson, T. Verstynen, J. M. Vettel, and S. F. Muldoon, Cognitive chimera states in human brain networks, *Sci. Adv.* 5(4), eaau8535 (2019)
9. P. Fries, A mechanism for cognitive dynamics: Neuronal communication through neuronal coherence, *Trends Cogn. Sci.* 9(10), 474 (2005)
10. J. F. Hipp, A. K. Engel, and M. Siegel, Oscillatory synchronization in large-scale cortical networks predicts perception, *Neuron* 69(2), 387 (2011)
11. T. J. Buschman and E. K. Miller, Top-down versus bottomup control of attention in the prefrontal and posterior parietal cortices, *Science* 315(5820), 1860 (2007)
12. J. Gross, F. Schmitz, I. Schnitzler, K. Kessler, K. Shapiro, B. Hommel, and A. Schnitzler, Modulation of long-range neural synchrony reflects temporal limitations of visual attention in humans, *Proc. Natl. Acad. Sci. USA* 101(35), 13050 (2004)
13. F. Crick and C. Koch, Some reflections on visual awareness, *Cold Spring Harb. Symp. Quant. Biol.* 55(0), 953 (1990)
14. M. Volgushev, S. Chauvette, M. Mukovski, and I. Timofecv, Precise long-range synchronization of activity and silence in neoconical neurons during slow-wave sleep, *J. Neurosci.* 26(21), 5665 (2006)
15. L. M. Ward, Synchronous neural oscillations and cognitive processes, *Trends Cogn. Sci.* 7(12), 553 (2003)
16. E. Bullmore and O. Sporns, The economy of brain network organization, *Nat. Rev. Neurosci.* 13(5), 336 (2012)
17. K. Bansal, J. D. Medaglia, D. S. Bassett, J. M. Vettel, and S. F. Muldoon, Data-driven brain network models differentiate variability across language tasks, *PLoS Comput. Biol.* 14(10), e1006487 (2018)
18. P. Hagmann, L. Cammoun, X. Gigandet, R. Meuli, C. J. Honey, J. V. Wedeen, and O. Sporns, Mapping the structural core of human cerebral cortex, *PLoS Biol.* 6(7), e159 (2008)
19. S. B. Eickhoff, B. T. T. Yeo, and S. Genon, Imaging-based parcellations of the human brain, *Nat. Rev. Neurosci.* 19(11), 672 (2018)
20. C. J. Honey, O. Sporns, L. Cammoun, X. Gigandet, J. P. Thiran, R. Meuli, and P. Hagmann, Predicting human resting-state functional connectivity from structural connectivity, *Proc. Natl. Acad. Sci. USA* 106(6), 2035 (2009)
21. S. Huo, C. Tian, M. Zheng, S. Guan, C. Zhou, and Z. Liu, Spatial multi-scaled chimera states of cerebral cortex network and its inherent structure dynamics relationship in human brain, *Natl. Sci. Rev.* 8(1), nwaa125 (2021)
22. C. J. Stam, Characterization of anatomical and functional connectivity in the brain: A complex networks perspective, *Int. J. Psychophysiol.* 77(3), 186 (2010)
23. O. Sporns, D. R. Chialvo, M. Kaiser, and C. C. Hilgetag, Organization, development and function of complex brain networks, *Trends Cogn. Sci.* 8(9), 418 (2004)
24. V. M. Eguíluz, D. R. Chialvo, G. A. Cecchi, M. Baliki, and A. V. Apkarian, Scale-free brain functional networks, *Phys. Rev. Lett.* 94(1), 018102 (2005)
25. D. S. Bassett, A. Meyer-Lindenberg, S. Achard, T. Duke, and E. Bullmore, Adaptive reconfiguration of fractal smallworld human brain functional networks, *Proc. Natl. Acad. Sci. USA* 103(51), 19518 (2006)
26. A. K. Engel, P. Fries, and W. Singer, Dynamic predictions: Oscillations and synchrony in top-down processing, *Nat. Rev. Neurosci.* 2(10), 704 (2001)
27. F. Varela, J. P. Lachaux, E. Rodriguez, and J. Martinerie, The Brainweb: Phase Synchronization and Large-Scale Integration, *Nat. Rev. Neurosci.* 2(4), 229 (2001)
28. K. E. Stephan, C. C. Hilgetag, G. A. P. C. Burns, M. A. O'Neill, M. P. Young, and R. Kotter, Computational analysis of functional connectivity between areas of primate cerebral cortex, *Philos. Trans. R. Soc. Lond. B* 355(1393), 111 (2000)
29. L. M. A. Bettencourt, G. J. Stephens, M. I. Ham, and G. W. Gross, Functional structure of cortical neuronal networks grown in vitro, *Phys. Rev. E* 75(2), 021915 (2007)
30. M. Guye, G. Bettus, F. Bartolomei, and P. J. Cozzone, Graph theoretical analysis of structural and functional connectivity MRI in normal and pathological brain networks, *MAGMA* 23(5–6), 409 (2010)
31. C. J. Stam, B. F. Jones, G. Nolte, M. Breakspear, and P. Scheltens, Small world networks and functional connectivity in Alzheimers disease, *Cereb. Cortex* 17(1), 92 (2006)
32. M. Chavez, M. Valencia, V. Navarro, V. Latora, and J. Martinerie, Functional modularity of background activities in normal and epileptic brain networks, *Phys. Rev. Lett.* 104(11), 118701 (2010)

33. M. Lynall, D. S. Bassett, R. Kerwin, P. J. McKenna, M. Kitzbichler, U. Muller, and E. Bullmore, Functional connectivity and brain networks in schizophrenia, *J. Neurosci.* 30(28), 9477 (2010)
34. K. J. Friston, Functional and effective connectivity in neuroimaging: A synthesis, *Hum. Brain Mapp.* 2(1–2), 56 (1994)
35. S. Boccaletti, J. Kurths, G. Osipov, D. L. Valladares, and C. S. Zhou, The synchronization of chaotic systems, *Phys. Rep.* 366(1–2), 1 (2002)
36. A. Pikovsky, M. Rosenblum, and J. Kurths, Synchronization: A Universal Concept in Nonlinear Sciences, Cambridge University Press, Cambridge, UK, 2001
37. A. Arenas, A. Diaz-Guilera, J. Kurths, Y. Moreno, and C. Zhou, Synchronization in complex networks, *Phys. Rep.* 469(3), 93 (2008)
38. J. Fell and N. Axmacher, The role of phase synchronization in memory processes, *Nat. Rev. Neurosci.* 12(2), 105 (2011)
39. P. Sauseng, W. Klimesch, M. Doppelmayr, S. Hanslmayr, M. Schabus, and W. R. Gruber, Theta coupling in the human electroencephalogram during a working memory task, *Neurosci. Lett.* 354(2), 123 (2004)
40. J. Sarnthein, H. Petsche, P. Rappelsberger, G. L. Shaw, and A. von Stein, Synchronization between prefrontal and posterior association cortex during human working memory, *Proc. Natl. Acad. Sci. USA* 95(12), 7092 (1998)
41. N. Axmacher, D. P. Schmitz, T. Wagner, C. E. Elger, and J. Fell, Interactions between medial temporal lobe, prefrontal cortex, and inferior temporal regions during visual working memory, a combined intracranial EEG and functional magnetic resonance imaging study, *J. Neurosci.* 28(29), 7304 (2008)
42. P. Sauseng, W. Klimesch, K. F. Heise, W. R. Gruber, E. Holz, A. A. Karim, M. Glennon, C. Gerloff, N. Birbaumer, and F. C. Hummel, Brain oscillatory substrates of visual shortterm memory capacity, *Curr. Biol.* 19(21), 1846 (2009)
43. M. I. Rabinovich, A. N. Simmons, and P. Varona, Dynamical bridge between brain and mind, *Trends Cogn. Sci.* 19(8), 453 (2015)
44. H. R. Wilson and J. D. Cowan, Excitatory and inhibitory interactions in localized populations of model neurons, *Biophys. J.* 12(1), 1 (1972)
45. S. F. Muldoon, F. Pasqualetti, S. Gu, M. Cieslak, S. T. Grafton, J. M. Vettel, and D. S. Bassett, Stimulation-based control of dynamic brain networks, *PLoS Comput. Biol.* 12(9), e1005076 (2016)
46. F. Wendling, J. J. Bellanger, F. Bartolomei, and P. Chauvel, Relevance of nonlinear lumped-parameter models in the analysis of depth-EEG epileptic signals, *Biol. Cybern.* 83(4), 367 (2000)
47. C. Zhou, L. Zemanova, G. Zamora-Lopez, C. C. Hilgetag, and J. Kurths, StructureCfunction relationship in complex brain networks expressed by hierarchical synchronization, *New J. Phys.* 9(6), 178 (2007)
48. O. David, L. Harrison, and K. J. Friston, Modelling event-related responses in the brain, *Neuroimage* 25(3), 756 (2005)
49. J. M. Huntenburg, P. L. Bazin, and D. S. Margulies, Large-scale gradients in human cortical organization, *Trends Cogn. Neurosci.* 22, 21 (2018)
50. T. Ito, K. R. Kulkarni, D. H. Schultz, R. D. Mill, R. H. Chen, L. I. Solomyak, and M. W. Cole, Cognitive task information is transferred between brain regions via resting-state network topology, *Nat. Commun.* 8(1), 1027 (2017)
51. X. G. Wang, Synchronous patterns in complex networks, *Sci. Sin. Phys. Mech.* & *Astron.* 50, 010503 (2020)
52. M. L. Kelly, R. A. Peters, R. K. Tisdale, and J. A. Lesku, Unihemispheric sleep in crocodilians? *J. Exp. Biol.* 218(20), 3175 (2015)
53. N. C. Rattenborg, S. L. Lima, and C. J. Amlaner, Half-awake to the risk of predation, *Nature* 397(6718), 397 (1999)
54. N. C. Rattenborg, C. J. Amlaner, and S. L. Lima, Behavioral, neurophysiological and evolutionary perspectives on unihemispheric sleep, *Neurosci. Biobehav. Rev.* 24(8), 817 (2000)
55. M. Tamaki, J. W. Bang, T. Watanabe, and Y. Sasaki, Night watch in one brain hemisphere during sleep associated with the first-night effect in humans, *Curr. Biol.* 26(9), 1190 (2016)
56. D. M. Abrams and S. H. Strogatz, Chimera states for coupled oscillators, *Phys. Rev. Lett.* 93(17), 174102 (2004)
57. M. J. Panaggio and D. M. Abrams, Chimera states: Coexistence of coherence and incoherence in networks of coupled oscillators, *Nonlinearity* 28(3), R67 (2015)
58. S. Majhi, B. K. Bera, D. Ghosh, and M. Perc, Chimera states in neuronal networks: A review, *Phys. Life Rev.* 28, 100 (2019)
59. Z. Wang and Z. Liu, Partial synchronization in complex networks: Chimera state, remote synchronization, and cluster synchronization, *Acta Physica Sinica* 69(8), 088902 (2020)
60. Z. Wang and Z. Liu, A brief review of chimera state in empirical brain networks, *Front. Physiol.* 11, 724 (2020)
61. R. Ma, J. Wang, and Z. Liu, Robust features of chimera states and the implementation of alternating chimera states, *Europhys. Lett.* 91(4), 40006 (2010)
62. Y. Zhu, Z. Zheng, and J. Yang, Chimera states on complex networks, *Phys. Rev. E* 89(2), 022914 (2014)
63. T. Chouzouris, I. Omelchenko, A. Zakharova, J. Hlinka, P. Jiruska, and E. Schöll, Chimera states in brain networks: Empirical neural vs. modular fractal connectivity, *Chaos* 28(4), 045112 (2018)
64. R. G. Andrzejak, C. Rummel, F. Mormann, and K. Schindler, All together now: Analogies between chimera state collapses and epileptic seizures, *Sci. Rep.* 6(1), 23000 (2016)
65. L. Kang, C. Tian, S. Huo, and Z. Liu, A two-layered brain network model and its chimera state, *Sci. Rep.* 9(1), 14389 (2019)
66. S. Huo, C. Tian, M. Zheng, S. Guan, C. S. Zhou, and Z. Liu, Spatial multi-scaled chimera states of cerebral cortex network and its inherent structure-dynamics relationship in human brain, *Natl. Sci. Rev.* 8(1), nwaa125 (2021)

67. R. Vicente, L. L. Gollo, C. R. Mirasso, I. Fischer, and G. Pipa, Dynamical relaying can yield zero time lag neuronal synchrony despite long conduction delays, *Proc. Natl. Acad. Sci. USA* 105(44), 17157 (2008)
68. P. R. Roelfsema, A. K. Engel, P. Konig, and W. Singer, Visuomotor integration is associated with zero time lag synchronization among cortical areas, *Nature* 385(6612), 157 (1997)
69. E. Rodriguez, N. George, J. P. Lachaux, J. Martinerie, B. Renault, and F. J. Varela, Perception's shadow: Long-distance synchronization of human brain activity, *Nature* 397(6718), 430 (1999)
70. V. Vuksanović and P. Hovel, Functional connectivity of distant cortical regions: Role of remote synchronization and symmetry in interactions, *Neuroimage* 97, 1 (2014)
71. A. Bergner, M. Frasca, G. Sciuto, A. Buscarino, E. J. Ngamga, L. Fortuna, and J. Kurths, Remote synchronization in star networks, *Phys. Rev. E* 85(2), 026208 (2012)
72. L. Kang, Z. Wang, S. Huo, C. Tian, and Z. Liu, Remote synchronization in human cerebral cortex network with identical oscillators, *Nonlinear Dyn.* 99(2), 1577 (2020)
73. M. A. Kramer and S. S. Cash, Epilepsy as a disorder of cortical network organization, *Neuroscientist* 18(4), 360 (2012)
74. M. Guye, J. Regis, M. Tamura, F. Wendling, A. Mc Gonigal, P. Chauvel, and F. Bartolomei, The role of corticothalamic coupling in human temporal lobe epilepsy, *Brain* 129(7), 1917 (2006)
75. Z. Wang, C. Tian, M. Dhamala, and Z. Liu, A small change in neuronal network topology can induce explosive synchronization transition and activity propagation in the entire network, *Sci. Rep.* 7(1), 561 (2017)
76. J. Gómez-Gardeñes, S. Gomez, A. Arenas, and Y. Moreno, Explosive synchronization transitions in scale-free networks, *Phys. Rev. Lett.* 106(12), 128701 (2011)
77. I. Leyva, R. Sevilla-Escoboza, J. M. Buldú, I. Sendiña-Nadal, J. Gómez-Gardeñes, A. Arenas, Y. Moreno, S. Gómez, R. Jaimes-Reátegui, and S. Boccaletti, Explosive first-order transition to synchrony in networked chaotic oscillators, *Phys. Rev. Lett.* 108(16), 168702 (2012)
78. P. Ji, T. K. D. M. Peron, P. J. Menck, F. A. Rodrigues, and J. Kurths, Cluster explosive synchronization in complex networks, *Phys. Rev. Lett.* 110(21), 218701 (2013)
79. X. Zhang, X. Hu, J. Kurths, and Z. Liu, Explosive synchronization in a general complex network, *Phys. Rev. E* 88, 010802(R) (2013)
80. Y. Zou, T. Pereira, M. Small, Z. Liu, and J. Kurths, Basin of attraction determines hysteresis in explosive synchronization, *Phys. Rev. Lett.* 112(11), 114102 (2014)
81. X. Zhang, Y. Zou, S. Boccaletti, and Z. Liu, Explosive synchronization as a process of explosive percolation in dynamical phase space, *Sci. Rep.* 4(1), 5200 (2015)
82. X. Zhang, S. Boccaletti, S. Guan, and Z. Liu, Explosive synchronization in adaptive and multilayer networks, *Phys. Rev. Lett.* 114(3), 038701 (2015)
83. S. Boccaletti, J. A. Almendral, S. Guan, I. Leyva, Z. Liu, I. Sendiña-Nadal, Z. Wang, and Y. Zou, Explosive transitions in complex networks structure and dynamics: Percolation and synchronization, *Phys. Rep.* 660, 1 (2016)
84. M. B. Kelz, Y. Sun, J. Chen, Q. Cheng Meng, J. T. Moore, S. C. Veasey, S. Dixon, M. Thornton, H. Funato, and M. Yanagisawa, An essential role for orexins in emergence from general anesthesia, *Proc. Natl. Acad. Sci. USA* 105(4), 1309 (2008)
85. E. B. Friedman, Y. Sun, J. T. Moore, H. T. Hung, Q. C. Meng, P. Perera, W. J. Joiner, S. A. Thomas, R. G. Eckenhoff, A. Sehgal, and M. B. Kelz, A conserved behavioral state barrier impedes transitions between anesthetic-induced unconsciousness and wakefulness: Evidence for neural inertia, *PLoS One* 5(7), e11903 (2010)
86. W. J. Joiner, E. B. Friedman, H. T. Hung, K. Koh, M. Sowcik, A. Sehgal, and M. B. Kelz, Genetic and anatomical basis of the barrier separatingwakefulness and anesthetic-induced unresponsiveness, *PLoS Genet.* 9(9), e1003605 (2013)
87. M. Kim, G. A. Mashour, S. B. Moraes, G. Vanini, V. Tarnal, E. Janke, A. G. Hudetz, and U. Lee, Functional and topological conditions for explosive synchronization develop in human brain networks with the onset of anesthetic-induced unconsciousness, *Front. Comput. Neurosci.* 10, 1 (2016)
88. A. C. Neubauer and A. Fink, Intelligence and neural efficiency, *Neurosci. Biobehav. Rev.* 33(7), 1004 (2009)
89. E. Genç, C. Fraenz, C. Schlüter, P. Friedrich, R. Hossiep, M. C. Voelkle, J. M. Ling, O. Güntürkün, and R. E. Jung, Diffusion markers of dendritic density and arborization in gray matter predict differences in intelligence, *Nat. Commun.* 9(1), 1905 (2018)
90. Y. Chen, S. Wang, C. C. Hilgetag, and C. Zhou, Trade-off between multiple constraints enables simultaneous formation of modules and hubs in neural systems, *PLoS Comput. Biol.* 9(3), e1002937 (2013)
91. M. Kaiser and C. Hilgetag, Nonoptimal component placement, but short processing paths, due to long-distance projections in neural systems, *PLoS Comput. Biol.* 2(7), e95 (2006)
92. J. Budd, K. Kovács, A. S. Ferecskó, P. Buzás, U. T. Eysel, and Z. F. Kisvárday, Neocortical axon arbors trade-off material and conduction delay conservation, *PLoS Comput. Biol.* 6(3), e1000711 (2010)
93. S. Baron-Cohen, R. C. Knickmeyer, and M. K. Belmonte, Sex differences in the brain: Implications for explaining autism, *Science* 310(5749), 819 (2005)
94. I. J. Deary, L. Penke, and W. Johnson, The neuroscience of human intelligence differences, *Nat. Rev. Neurosci.* 11(3), 201 (2010)
95. L. Cao and Z. Liu, How IQ depends on the running mode of brain network? *Chaos* 30(7), 073111 (2020)
96. J. Wang and Z. Liu, A chain model for signal detection and transmission, *Europhys. Lett.* 102(1), 10003 (2013)
97. Z. Liu, Organization network enhanced detection and transmission of phase–locking, *Europhys. Lett.* 100(6), 60002 (2012)
98. Q. Shen and Z. Liu, Remote firing propagation in the neural network of *C. elegans*, *Phys. Rev. E* 103(5), 052414 (2021)

99. Z. Wang and Z. Liu, Effect of remote signal propagation in an empirical brain network, *Chaos* 31(6), 063126 (2021)

100. I. Diez, A. Erramuzpe, I. Escudero, B. Mateos, A. Cabrera, D. Marinazzo, E. J. Sanz-Arigita, S. Stramaglia, and J. M. Cortes Diaz, Information flow between resting-state networks, *Brain Connect.* 5(9), 554 (2015)

101. M. R. Brier, J. B. Thomas, A. Z. Snyder, T. L. Benzinger, D. Zhang, M. E. Raichle, D. M. Holtzman, J. C. Morris, and B. M. Ances, Loss of intranetwork and internetwork resting state functional connections with Alzheimer's disease progression, *J. Neurosci.* 32(26), 8890 (2012)

102. E. J. Sanz-Arigita, M. M. Schoonheim, J. S. Damoiseaux, S. A. R. B. Rombouts, E. Maris, F. Barkhof, P. Scheltens, and C. J. Stam, Loss of 'small-world' networks in Alzheimer's disease: Graph analysis of fMRI resting-state functional connectivity, *PLoS One* 5(11), e13788 (2010)

103. E. Başar, C. Basar-Eroglu, S. Karakas, and M. Schurmann, Gamma, alpha, delta, and theta oscillations govern cognitive processes, *Int. J. Psychophysiol.* 39(2–3), 241 (2001)

104. E. Bullmore and O. Sporns, Complex brain networks: Graph theoretical analysis of structural and functional systems, *Nat. Rev. Neurosci.* 10(3), 186 (2009)

105. R. Wang, P. Lin, M. Liu, Y. Wu, T. Zhou, and C. Zhou, Hierarchical connectome modes and critical state jointly maximize human brain functional diversity, *Phys. Rev. Lett.* 123(3), 038301 (2019)